

C₂-Symmetric Bis(oxazolinato)lanthanide Catalysts for Enantioselective Intramolecular Hydroamination/Cyclization

Sukwon Hong, Shun Tian, Matthew V. Metz, and Tobin J. Marks*

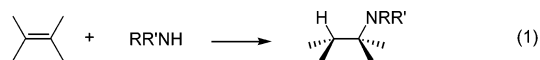
Contribution from the Department of Chemistry, Northwestern University, 2145 Sheridan Road, Evanston, Illinois 60208-3113

Received June 2, 2003; E-mail: t-marks@northwestern.edu

Abstract: C₂-symmetric bis(oxazolinato)lanthanide complexes of the type [(4*R*,5*S*)-Ph₂Box]La[N(TMS)₂]₂, [(4*S*,5*R*)-Ar₂Box]La[N(TMS)₂]₂, and [(4*S*)-Ph-5,5-Me₂Box]La[N(TMS)₂]₂ (Box = 2,2'-bis(2-oxazoline)methylenyl; Ar = 4-*tert*-butylphenyl, 1-naphthyl; TMS = SiMe₃) serve as precatalysts for the efficient enantioselective intramolecular hydroamination/cyclization of aminoalkenes and aminodienes. These new catalyst systems are conveniently generated in situ from the known metal precursors Ln[N(TMS)₂]₃ or Ln[CH(TMS)₂]₃ (Ln = La, Nd, Sm, Y, Lu) and 1.2 equiv of commercially available or readily prepared bis(oxazoline) ligands such as (4*R*,5*S*)-Ph₂BoxH, (4*S*,5*R*)-Ar₂BoxH, and (4*S*)-Ph-5,5-Me₂BoxH. The X-ray crystal structure of [(4*S*)-*t*-BuBox]Lu[CH(TMS)₂]₂ provides insight into the structure of the in situ generated precatalyst species. Lanthanides having the largest ionic radii exhibit the highest turnover frequencies as well as enantioselectivities. Reaction rates maximize near 1:1 BoxH:Ln ratio (ligand acceleration); however, increasing the ratio to 2:1 BoxH:Ln decreases the reaction rate, while affording enantiomeric excesses similar to the 1:1 BoxH:Ln case. A screening study of bis(oxazoline) ligands reveals that aryl stereodirecting groups at the oxazoline ring 4 position and additional substitution (geminal dimethyl or aryl) at the 5 position are crucial for high turnover frequencies and good enantioselectivities. The optimized precatalyst, in situ generated [(4*R*,5*S*)-Ph₂Box]La[N(TMS)₂]₂, exhibits good rates and enantioselectivities, comparable to or greater than those achieved with chiral C₁-symmetric organolanthanocene catalysts, even for poorly responsive substrates (up to 67% ee at 23 °C). Kinetic studies reveal that hydroamination rates are zero order in [amine substrate] and first order in [catalyst], implicating the same general mechanism for organolanthanide-catalyzed hydroamination/cyclizations (intramolecular turnover-limiting olefin insertion followed by the rapid protonolysis of an Ln–C bond by amine substrate) and implying that the active catalytic species is monomeric.

Introduction

Catalytic asymmetric synthesis¹ represents the forefront of modern synthetic organic and organometallic chemistry. The ability to produce large quantities of desired, enantiomerically pure compounds from simple feedstocks and relatively small quantities of enantioenriched catalysts has spectacular practical implications. Hydroamination,² the formal addition of an N–H bond across carbon–carbon unsaturation, has attracted much recent attention,^{3–7} because it offers an efficient, atom-economical route to nitrogen-containing molecules which are important for fine chemicals, pharmaceuticals, useful chiral building blocks, or chiral ligands in asymmetric catalysis (eq 1).

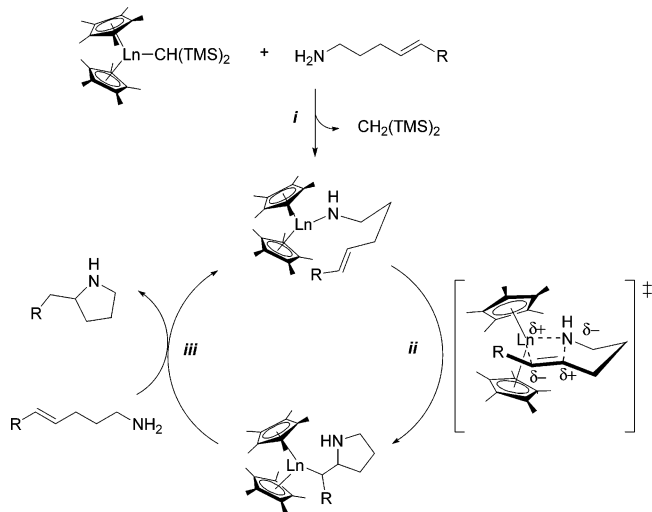


Especially *enantioselective hydroamination*^{3,8,9,10a} using chiral catalysts is one of the most desirable, elegant transformations, enabling the synthesis of chiral amines from simple, readily available prochiral substrates in a single step. Organolanthanides¹¹ are highly efficient catalysts for the inter-¹² and intramolecular hydroamination/cyclization of diverse C–C unsaturated functionalities such as aminoalkenes,^{8,9,13} aminoalkynes,¹⁴ aminoallenes,¹⁵ and aminodienes¹⁰ (e.g., Scheme 1). Attractive features of organolanthanide catalysts include very high turnover frequencies and excellent diastereoselectivities, rendering this methodology readily applicable to the synthesis of complex alkaloids and other organonitrogen molecules.^{15a}

- (1) (a) Sharpless, K. B. *Angew. Chem., Int. Ed.* **2002**, *41*, 2024–2032 (2002 Nobel lecture). (b) *Acc. Chem. Res.* **2000**, *6*, 323–440 (Special Asymmetric Catalysis Issue, Denmark, S. E., Jacobsen E. N., Eds.). (c) Ojima, I., Ed. *Catalytic Asymmetric Synthesis*; VCH: New York, 2000. (d) Jacobsen, E. N., Pfaltz, A., Yamamoto, H., Eds. *Comprehensive Asymmetric Catalysis*; Springer: Berlin, 1999; Vol. 1–III. (e) Noyori, R. *Asymmetric Catalysis in Organic Synthesis*; John Wiley & Sons: New York, 1994.
- (2) For recent reviews of catalytic hydroamination, see: (a) Pohlki, F.; Doye, S. *Chem. Soc. Rev.* **2003**, *32*, 104–114. (b) Bytschkov, I.; Doye, S. *Eur. J. Org. Chem.* **2003**, 935–946. (c) Nobis, M.; Driessen-Hölscher, B. *Angew. Chem., Int. Ed.* **2001**, *40*, 3983–3985. (d) Brunet, J. J.; Neibecker, D. In *Catalytic Heterofunctionalization*; Togni, A., Grützmacher, H., Eds.; Wiley-VCH: Weinheim, 2001; pp 91–141. (e) Müller, T. E.; Beller, M. *Chem. Rev.* **1998**, *98*, 675–703.

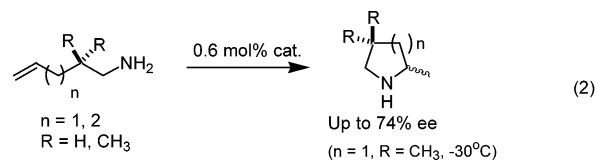
- (3) For recent examples of *enantioselective hydroamination* catalyzed by chiral late transition metal complexes, see: (a) Li, K.; Horton, P. N.; Hursthouse, M. B.; Hii, K. K. M. *J. Organomet. Chem.* **2003**, *665*, 250–257. (b) Fadini, L.; Togni, A. *Chem. Commun.* **2003**, 30–31. (c) Pawlas, J.; Nakao, Y.; Kawatsura, M.; Hartwig, J. F. *J. Am. Chem. Soc.* **2002**, *124*, 3669–3679. (d) Löber, O.; Kawatsura, M.; Hartwig, J. F. *J. Am. Chem. Soc.* **2001**, *123*, 4366–4367. (e) Kawatsura, M.; Hartwig, J. F. *J. Am. Chem. Soc.* **2000**, *122*, 9546–9547. (f) Vasen, D.; Salzer, A.; Gerhards, F.; Gais, H.-J.; Stürmer, R.; Bieler, N. H.; Togni, A. *Organometallics* **2000**, *19*, 539–546. (g) Dorta, R.; Egli, P.; Zürcher, F.; Togni, A. *J. Am. Chem. Soc.* **1997**, *119*, 10857–10858.

Scheme 1. Simplified Catalytic Cycle for Organolanthanide-Mediated Hydroamination/Cyclization of Aminoalkenes



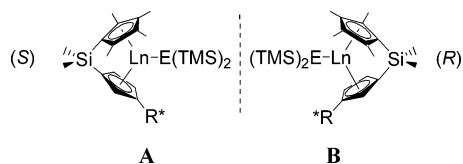
Thus, there has been a growing interest in developing chiral organolanthanide complexes to combine the unique catalytic properties of lanthanides with a chiral coordination sphere.¹⁶ In the early 1990s, the first enantioselective intramolecular

hydroamination was reported for a limited group of substrates using C₁-symmetric chiral organolanthanide complexes (eq 2).^{8d}

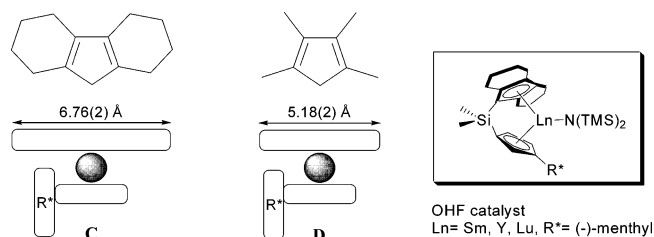


Ansa-lanthanocene frameworks were modified by incorporating a chiral moiety, an R* such as (–)-menthyl, (–)-phenylmenthyl, or (+)-neomenthyl, to ensure the formation of separable, diastereomeric complexes of the type Me₂Si(Cp'')(CpR*)LnE-(TMS)₂ (Cp'' = η⁵-Me₄C₅; Cp = η⁵-C₅H₅; Ln = La, Sm, Y, Lu; R* = (+)-neomenthyl, (–)-menthyl; E = N, CH; TMS = SiMe₃; **A**, **B**).^{8b–d,17} The bulky nature of R* and the size differences between the “upper” (C₅Me₄–) and “lower” (R*–C₅H₅–) Cp rings are designed to provide lateral and transverse

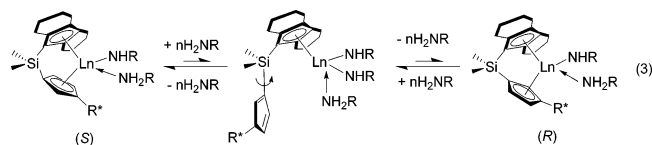
- (4) For recent examples of hydroamination catalyzed by achiral late transition metal complexes, see: (a) Shimada, T.; Yamamoto, Y. *J. Am. Chem. Soc.* **2002**, *124*, 12670–12671. (b) Neff, V.; Müller, T. E.; Lercher, J. A. *Chem. Commun.* **2002**, 906–907. (c) Lutete, L. M.; Kadota, I.; Shibuya, A.; Yamamoto, Y. *Heterocycles* **2002**, *58*, 347–357. (d) Nettekoven, U.; Hartwig, J. F. *J. Am. Chem. Soc.* **2002**, *124*, 1166–1167. (e) Minami, T.; Okamoto, H.; Ikeda, S.; Tanaka, R.; Ozawa, F.; Yoshifuji, M. *Angew. Chem., Int. Ed.* **2001**, *40*, 4501–4503. (f) Hartung, C. G.; Tillack, A.; Trauthwein, H.; Beller, M. *J. Org. Chem.* **2001**, *66*, 6339–6343. (g) Müller, T. E.; Berger, M.; Grosche, M.; Herdtweck, E.; Schmidtchen, F. P. *Organometallics* **2001**, *20*, 4384–4393. (h) Kawatsura, M.; Hartwig, J. F. *Organometallics* **2001**, *20*, 1960–1964. (i) Senn, H. M.; Blöchl, P. E.; Togni, A. *J. Am. Chem. Soc.* **2000**, *122*, 4098–4107. (j) Müller, T. E.; Grosche, M.; Herdtweck, E.; Pleier, A.-K.; Walter, E.; Yan, Y.-K. *Organometallics* **2000**, *19*, 170–183. (k) Burling, S.; Field, L. D.; Messerle, B. A. *Organometallics* **2000**, *19*, 87–90. (l) Kadota, I.; Shibuya, A.; Lutete, L. M.; Yamamoto, Y. *J. Org. Chem.* **1999**, *64*, 4570–4571. (m) Tokunaga, M.; Eckert, M.; Wakatsuki, Y. *Angew. Chem., Int. Ed.* **1999**, *38*, 3222–3225. (n) Uchimar, Y. *Chem. Commun.* **1999**, 1133–1134. (o) Beller, M.; Trauthwein, H.; Eichberger, M.; Breindl, C.; Müller, T. E. *Eur. J. Inorg. Chem.* **1999**, 1121–1132. (p) Beller, M.; Trauthwein, H.; Eichberger, M.; Breindl, C.; Herwig, J.; Müller, T. E.; Thiel, O. R. *Chem.-Eur. J.* **1999**, *5*, 1306–1319. (q) Nakamura, I.; Itagaki, H.; Yamamoto, Y. *J. Org. Chem.* **1998**, *63*, 6458–6459. (r) Meguro, M.; Yamamoto, Y. *Tetrahedron Lett.* **1998**, *39*, 5421–5424. (s) Radhakrishnan, U.; Al-Masum, M.; Yamamoto, Y. *Tetrahedron Lett.* **1998**, *39*, 1037–1040.
- (5) For recent examples of hydroamination catalyzed by early transition metals, see: (a) Castro, I. G.; Tillack, A.; Hartung, C. G.; Beller, M. *Tetrahedron Lett.* **2003**, *44*, 3217–3221. (b) Shi, Y.; Hall, C.; Ciszewski, J. T.; Cao, C.; Odom, A. L. *Chem. Commun.* **2003**, 586–587. (c) Tillack, A.; Castro, I. G.; Hartung, C. G.; Beller, M. *Angew. Chem., Int. Ed.* **2002**, *41*, 2541–2543. (d) Cao, C.; Shi, Y.; Odom, A. L. *Org. Lett.* **2002**, *4*, 2853–2856. (e) Ong, T.-G.; Yap, G. P. A.; Richeson, D. S. *Organometallics* **2002**, *21*, 2839–2841. (f) Pohlki, F.; Heutling, A.; Bytschkov, I.; Hotopp, T.; Doye, S. *Synlett* **2002**, 799–801. (g) Ackermann, L.; Bergman, R. G. *Org. Lett.* **2002**, *4*, 1475–1478. (h) Heutling, A.; Doye, S. *J. Org. Chem.* **2002**, *67*, 1961–1964. (i) Haak, E.; Bytschkov, I.; Doye, S. *Eur. J. Org. Chem.* **2002**, 457–463. (j) Siebeneicher, H.; Doye, S. *Eur. J. Org. Chem.* **2002**, 1213–1220. (k) Bytschkov, I.; Doye, S. *Tetrahedron Lett.* **2002**, *43*, 3715–3718. (l) Bytschkov, I.; Doye, S. *Eur. J. Org. Chem.* **2001**, 4411–4418. (m) Straub, B. F.; Bergman, R. G. *Angew. Chem., Int. Ed.* **2001**, *40*, 4632–4635. (n) Cao, C.; Ciszewski, J. T.; Odom, A. L. *Organometallics* **2001**, *20*, 5011–5013. (o) Johnson, J. S.; Bergman, R. G. *J. Am. Chem. Soc.* **2001**, *123*, 2923–2924. (p) Shi, Y.; Ciszewski, J. T.; Odom, A. L. *Organometallics* **2001**, *20*, 3967–3969. (q) Pohlki, F.; Doye, S. *Angew. Chem., Int. Ed.* **2001**, *40*, 2305–2308. (r) Haak, E.; Siebeneicher, H.; Doye, S. *Org. Lett.* **2000**, *2*, 1935–1937. (s) Haak, E.; Bytschkov, I.; Doye, S. *Angew. Chem., Int. Ed.* **1999**, *38*, 3389–3391. (t) Duncan, D.; Livinghouse, T. *Organometallics* **1999**, *18*, 4421–4428.
- (6) For recent examples of hydroamination catalyzed by actinide metals, see: (a) Wang, J.; Dash, A. K.; Kapon, M.; Berthet, J.-C.; Ephritikhine, M.; Eisen, M. S. *Chem.-Eur. J.* **2002**, *8*, 5384–5396. (b) Straub, T.; Haskel, A.; Neyroud, T. G.; Kapon, M.; Botoshansky, M.; Eisen, M. S. *Organometallics* **2001**, *20*, 5017–5035. (c) Haskel, A.; Straub, T.; Eisen, M. S. *Organometallics* **1996**, *15*, 3773–3775.
- (7) For recent examples of base-catalyzed hydroaminations, see: (a) Trost, B. M.; Tang, W. J. *J. Am. Chem. Soc.* **2002**, *124*, 14542–14543. (b) Hartung, C. G.; Breindl, C.; Tillack, A.; Beller, M. *Tetrahedron* **2000**, *56*, 5157–5162. (c) Beller, M.; Breindl, C.; Riermeier, T. H.; Eichberger, M.; Trauthwein, H. *Angew. Chem., Int. Ed.* **1998**, *37*, 3389–3391. For recent examples of acid-catalyzed hydroaminations, see: (d) Schlummer, B.; Hartwig, J. F. *Org. Lett.* **2002**, *4*, 1471–1474. (e) Miura, K.; Hondo, T.; Nakagawa, T.; Takahashi, T.; Hosomi, A. *Org. Lett.* **2000**, *2*, 385–388.
- (8) (a) Douglass, M. R.; Ogasawara, M.; Hong, S.; Metz, M. V.; Marks, T. J. *Organometallics* **2002**, *21*, 283–292. (b) Giardello, M. A.; Conticello, V. P.; Brard, L.; Gagné, M. R.; Marks, T. J. *J. Am. Chem. Soc.* **1994**, *116*, 10241–10254. (c) Giardello, M. A.; Conticello, V. P.; Brard, L.; Sabat, M.; Rheingold, A. L.; Stern, C. L.; Marks, T. J. *J. Am. Chem. Soc.* **1994**, *116*, 10212–10240. (d) Gagné, M. R.; Brard, L.; Conticello, V. P.; Giardello, M. A.; Stern, C. L.; Marks, T. J. *Organometallics* **1992**, *11*, 2003–2005.
- (9) O'Shaughnessy, P. N.; Knight, P. D.; Morton, C.; Gillespie, K. M.; Scott, P. *Chem. Commun.* **2003**, 1770–1771.
- (10) (a) Hong, S.; Marks, T. J. *J. Am. Chem. Soc.* **2002**, *124*, 7886–7887. (b) Hong, S.; Kawaoka, A. M.; Marks, T. J. *J. Am. Chem. Soc.*, in press.
- (11) For organolanthanide reviews, see: (a) Aspinall, H. C. *Chem. Rev.* **2002**, 1807–1850. (b) Edelmann, F. T.; Freckmann, D. M. M.; Schumann, H. *Chem. Rev.* **2002**, 1851–1896. (c) Arndt, S.; Okuda, J. *Chem. Rev.* **2002**, 1953–1976. (d) Molander, G. A.; Romero, J. A. C. *Chem. Rev.* **2002**, 2161–2185. (e) *Topics in Organometallic Chemistry*; Kobayashi, S., Ed.; Springer: Berlin, 1999; Vol. 2. (f) Edelmann, F. T. *Top. Curr. Chem.* **1996**, *179*, 247–276. (g) Schumann, H.; Meese-Marktscheffel, J. A.; Esser, L. *Chem. Rev.* **1995**, *95*, 865–986. (h) Schaverien, C. J. *Adv. Organomet. Chem.* **1994**, *36*, 283–362.
- (12) (a) Ryu, J.-S.; Li, G. Y.; Marks, T. J. *J. Am. Chem. Soc.* **2003**, *125*, 12584–12605. (b) Li, Y.; Marks, T. J. *Organometallics* **1996**, *15*, 3770–3772.
- (13) (a) Kim, Y. K.; Livinghouse, T. *Angew. Chem., Int. Ed.* **2002**, *41*, 3645–3647. (b) Ryu, J.-S.; Marks, T. J.; McDonald, F. E. *Org. Lett.* **2001**, *3*, 3091–3094. (c) Molander, G. A.; Dowdy, E. D.; Pack, S. K. *J. Org. Chem.* **2001**, *66*, 4344–4347. (d) Kim, Y. K.; Livinghouse, T.; Bercaw, J. E. *Tetrahedron Lett.* **2001**, *42*, 2933–2935. (e) Molander, G. A.; Dowdy, E. D. *J. Org. Chem.* **1999**, *64*, 6515–6517. (f) Tian, S.; Arredondo, V. M.; Stern, C. L.; Marks, T. J. *Organometallics* **1999**, *18*, 2568–2570. (g) Gilbert, A. T.; Davis, B. L.; Emge, T. J.; Broene, R. D. *Organometallics* **1999**, *18*, 2125–2132. (h) Molander, G. A.; Dowdy, E. D. *J. Org. Chem.* **1998**, *63*, 8983–8988. (i) Gagné, M. R.; Stern, C. L.; Marks, T. J. *J. Am. Chem. Soc.* **1992**, *114*, 275–294. (j) Gagné, M. R.; Nolan, S. P.; Marks, T. J. *Organometallics* **1990**, *9*, 1716–1718. (k) Gagné, M. R.; Marks, T. J. *J. Am. Chem. Soc.* **1989**, *111*, 4108–4109.
- (14) (a) Li, Y.; Marks, T. J. *J. Am. Chem. Soc.* **1998**, *120*, 1757–1771. (b) Bürgstein, M. R.; Berberich, H.; Roesky, P. W. *Organometallics* **1998**, *17*, 1452–1454. (c) Li, Y.; Marks, T. J. *J. Am. Chem. Soc.* **1996**, *118*, 9295–9306. (d) Li, Y.; Marks, T. J. *J. Am. Chem. Soc.* **1996**, *118*, 707–708. (e) Li, Y.; Fu, P.-F.; Marks, T. J. *Organometallics* **1994**, *13*, 439–440.
- (15) (a) Arredondo, V. M.; Tian, S.; McDonald, F. E.; Marks, T. J. *J. Am. Chem. Soc.* **1999**, *121*, 3633–3639. (b) Arredondo, V. M.; McDonald, F. E.; Marks, T. J. *Organometallics* **1999**, *18*, 1949–1960. (c) Arredondo, V. M.; McDonald, F. E.; Marks, T. J. *J. Am. Chem. Soc.* **1998**, *120*, 4871–4872.
- (16) For reviews of chiral lanthanide complexes, see: (a) ref 11a. (b) Mikami, K.; Terada, M.; Matsuzawa, H. *Angew. Chem., Int. Ed.* **2002**, *41*, 3554–3571.
- (17) Other asymmetric transformations with these catalysts include: (a) olefin hydrogenation (up to 96% ee); ref 8b,c. (b) hydrosilylation (up to 78% ee); Fu, P.-F.; Brard, L.; Li, Y.; Marks, T. J. *J. Am. Chem. Soc.* **1995**, *117*, 7157–7168. (c) isospecific methyl methacrylate polymerization (*mm* up to 94%); Giardello, M. A.; Yamamoto, Y.; Brard, L.; Marks, T. J. *J. Am. Chem. Soc.* **1995**, *117*, 3276–3277.



discrimination, respectively. Such catalysts are effective in the formation of five-membered rings via hydroamination/cyclization of aminoalkenes (up to 74% ee); however, the level of asymmetric induction falls precipitously (to 15–17% ee) in the formation of homologous six-membered rings. Later, the structural motif of these first-generation chiral C_1 -symmetric organolanthanides was further modified by increasing the “wing span” of the “upper” η^5 ligand to increase top–bottom ligand–substrate steric discrimination (**C** vs **D**). Thus, second-generation



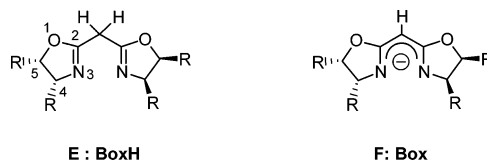
chiral C_1 -symmetric organolanthanides with a stereodemanding, electron-donating octahydrofluorenyl (OHF) top have recently been synthesized.^{8a} In comparison to the first-generation C_1 -symmetric catalysts, the OHF catalysts exhibit greater enantioselectivities in hydroamination with sterically encumbered six-membered ring substrates (up to 67% ee); however, only comparable or slightly lower enantioselectivities are observed in many other cases. Overall, these C_1 -symmetric chiral Cp-based catalysts show respectable activity and selectivity (especially in olefin hydrogenation,^{8b,c} hydrosilylation,^{17b} and polymerization^{17c}), but the C_1 -symmetric Cp-based ligand structures have several drawbacks. First, the epimerization of catalysts in the presence of amine molecules is observed for both C_1 -symmetric catalytic systems (eq 3).⁸ This intrinsic



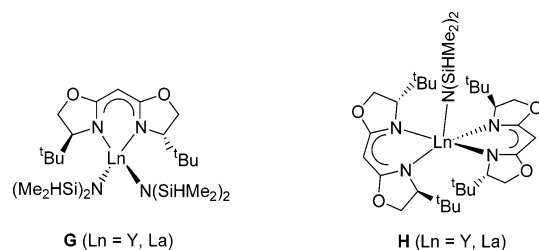
complexity not only contributes to lowered enantioselectivity but also hampers accessibility to both product enantiomers from each precatalyst isomer.¹⁸ Second, both catalyst antipode structures are not always straightforwardly accessible. The isolation/purification of such catalysts depends principally on fractional crystallization of diastereomeric mixtures, and the diastereomer ratio is controlled mainly by the choice of recrystallization solvent and temperature. Finally, these Cp-based systems are somewhat difficult to tune in terms of positioning stereodifferentiating groups.

To address the aforementioned issues, we embarked on the search for new, nonepimerizable chiral ligand designs for lanthanide-mediated hydroamination. For hydroaminations, the lanthanide precatalyst should have at least one labile ligand that can be protonolytically substituted by amines to form lanthanide

amido species (Scheme 1, step i).¹⁹ In addition, the stereodifferentiating ligands should be intact in the presence of a large excess of amine. We envisioned bis(oxazoline) (Box) ligands (**E**) as effective, nonepimerizable C_2 -symmetric ligands for lanthanides. Bis(oxazoline) ligands are some of the most



effective transition metal ligands for a variety of catalytic transformations,²⁰ and the chelating deprotonated, imido/amido bidentate ligands (**F**) should provide the required kinetic stability during the reaction. In fact, Anwender and co-workers recently communicated the synthesis of mono- and bis[bis(oxazolinato)]-lanthanide complexes (**G** and **H**, respectively), although no catalytic details have been reported since then.^{19c}



Herein, we report intramolecular hydroamination/cyclization processes mediated by a new series of chiral in situ generated C_2 -symmetric bis(oxazolinato)lanthanide complexes. The synthesis of variously substituted Box ligands, in situ generation of bis(oxazolinato)lanthanide catalysts of the type BoxLn-[N(TMS)₂]₂ (Box = deprotonated bisoxazoline), crystallographic characterization of one precatalyst, and an investigation of the catalytic properties with respect to intramolecular enantioselective aminoalkene and aminodiene cyclization are presented.²¹

Experimental Section

Materials and Methods. All manipulations of air-sensitive materials were carried out with rigorous exclusion of oxygen and moisture in flame- or oven-dried Schlenk-type glassware on a dual-manifold Schlenk line, interfaced to a high-vacuum line (10^{-6} Torr), or in a nitrogen-filled Vacuum Atmospheres glovebox with a high capacity recirculator (<1 ppm of O₂). Argon (Matheson, prepurified) was

- (18) It was observed that the configurations and optical purities of the products are insensitive to the optical purity/configuration of the precatalyst. Rapid epimerization was proposed to explain these phenomena. See ref 8b.
- (19) For examples of nonmetallocene chiral lanthanides with at least one dissociable ligand, see: (a) Lin, M.-H.; Rajanbabu, T. V. *Org. Lett.* **2002**, *4*, 1607–1610. (b) Giuseppone, N.; Santos, I.; Colin, J. *Tetrahedron Lett.* **2000**, *41*, 639–642. (c) Görlitzer, H. W.; Spiegler, M.; Anwender, R. *J. Chem. Soc., Dalton Trans.* **1999**, 4287–4288. (d) Gountchev, T. I.; Tilley, T. D. *Organometallics* **1999**, *18*, 2896–2905. (e) Görlitzer, H. W.; Spiegler, M.; Anwender, R. *Eur. J. Inorg. Chem.* **1998**, 1009–1014. (f) Schavieren, C. J.; Meijboom, N.; Orpen, A. G. *J. Chem. Soc., Chem. Commun.* **1992**, 124–126.
- (20) For recent reviews of chiral bis(oxazoline)–metal complexes, see: (a) Johnson, J. S.; Evans, D. A. *Acc. Chem. Res.* **2000**, *33*, 325–335. (b) Ghosh, A. K.; Mathivanan, P.; Cappiello, J. *Tetrahedron: Asymmetry* **1998**, *9*, 1–45.
- (21) Portions of this work were previously communicated: (a) Hong, S.; Ryu, J.-S.; Tian, S.; Metz, M. V.; Marks, T. J. *Abstract of Papers*; the 224th National ACS Meeting, Boston, MA, August 2002; American Chemical Society: Washington, DC, 2002; abstract INOR 668. (b) Hong, S.; Tian, S.; Metz, M. V.; Stern, C. L.; Marks, T. J. *Abstract of Papers*; the 222nd National ACS Meeting, Chicago, IL, August 2001; American Chemical Society: Washington, DC, 2001; abstract INOR 140.

purified by passage through a MnO oxygen-removal column and a Davison 4A molecular sieve column. Pentane and toluene were dried using activated alumina columns according to the method described by Grubbs²² and were additionally vacuum transferred from Na/K alloy immediately before use if employed for catalyst synthesis or catalytic reactions. Ether, THF, and dichloromethane were distilled before use from appropriate drying agents (sodium benzophenone ketyl, Na/K alloy, CaH₂, respectively) under nitrogen. Chloroform-*d* was purchased from Cambridge Isotope Laboratories. Benzene-*d*₆, toluene-*d*₈, cyclohexane-*d*₁₂, and methylcyclohexane-*d*₁₄ (Cambridge Isotope Laboratories; all 99+ atom % D) used for NMR reactions and kinetic measurements were stored in vacuo over Na/K alloy in resealable bulbs and were vacuum transferred immediately prior to use. All organic starting materials were purchased from Aldrich Chemical Co. or Lancaster Synthesis Inc. and were used without further purification unless otherwise stated. All bis(oxazoline) ligands either purchased from Aldrich or synthesized (see text), were degassed overnight on a high vacuum line and then stored in a glovebox. Substrates **11**,¹³ⁱ **15**,¹³ⁱ **17**,^{10a} **19**,^{8b} **21**,^{10a} and **23**^{10b} were prepared as reported previously. All substrates were dried twice as solutions in benzene-*d*₆ or toluene-*d*₈ over freshly activated Davison 4A molecular sieves and were degassed by freeze–pump–thaw methods. The substrates were then stored in vacuum-tight storage flasks. The lanthanide complexes Ln[N(TMS)₂]₃,²³ Ln[CH(TMS)₂]₃ (Ln = La, Sm, Y, Lu; TMS = SiMe₃),²⁴ (*R*)- or (*S*)-Me₂-SiCp''(CpR*)LnE(TMS)₂ (Cp'' = η^5 -C₅Me₄; Cp = η^5 -C₅H₃; R* = (–)-menthyl, (+)-neomenthyl, (–)-phenylmenthyl; Ln = Sm, Y; E = CH or N),^{8c} and (*S*)-Me₂Si(OHf)(CpR*)LnN(TMS)₂ (OHf = η^5 -octahydrofluorenyl; Cp = η^5 -C₅H₃; R* = (–)-menthyl; Ln = Sm, Y)^{8a} were prepared according to published procedures.

Physical and Analytical Measurements. NMR spectra were recorded on a Varian Gemini 300 (FT, 300 MHz, ¹H; 75 MHz, ¹³C), Unity- or Mercury-400 (FT, 400 MHz, ¹H; 100 MHz, ¹³C), or Inova-500 (FT, 500 MHz, ¹H; 125 MHz, ¹³C) instrument. Chemical shifts (δ) for ¹H and ¹³C are referenced to internal solvent resonances and reported relative to SiMe₄. NMR experiments on air-sensitive samples were conducted in Teflon valve-sealed tubes (J. Young). HRMS studies were conducted on a VG 70-250 SE instrument with 70 eV electron impact ionization or chemical ionization using isobutane as the reagent gas. Elemental analyses were performed by Midwest Microlabs, Indianapolis, IN or Oneida Research Services, Whitesboro, NY. GC-MS analyses were performed using an HP6890 instrument equipped with an HP5972 detector, an HP-5MS (5% Phenyl Methyl Siloxane, 30m \times 250 μ m \times 0.25 μ m) capillary column, and Chemstation software. HPLC analyses were performed using a Waters Breeze system consisting of a model 1525 binary pump, model 77251 manual injector, and model 2487 dual λ UV/vis detector. Optical rotations were measured using an Optical Activity AA-100 polarimeter. IR spectra were recorded using a Biorad FT S60 FTIR instrument.

(*S*)-2,2,2-Trifluoro-*N*-(2-hydroxy-2-methyl-1-phenylpropyl)acetamide (6a). Adapted from published procedure.²⁵ A solution of (*S*)-(+)-2-phenyl-*N*-(trifluoroacetyl)glycine methyl ester (purchased from Aldrich, 3.03 g, 11.6 mmol) in THF (40 mL) was added dropwise under N₂ to a methylmagnesium bromide (3 M in Et₂O, 19.5 mL, 58.5 mmol, 5.0 equiv) solution in THF (20 mL) over a period of 15 min. The reaction mixture was heated to reflux for 6 h and then was cooled to 0 °C before quenching with a saturated aqueous NH₄Cl solution (20 mL). H₂O (20 mL) was added, and the mixture was extracted with Et₂O (4 \times 50 mL). The combined organic extracts were washed with brine (50 mL), dried over MgSO₄, filtered, and concentrated to afford

a yellow oil. Purification by flash column chromatography (silica gel, hexanes:Et₂O = 1:1) provided 2.49 g (9.54 mmol, 82% yield) of the pure acetamide **6a** as a pale yellow crystalline solid. ¹H NMR (500 MHz, CDCl₃) δ 7.39–7.30 (m, 6 H), 4.80 (d, 9 Hz, 1 H), 1.53 (br s, 1 H), 1.39 (s, 3 H), 1.08 (s, 3 H); ¹³C NMR (125.6 MHz, CDCl₃) δ 157.0, 156.7, 137.6, 128.8, 128.5, 128.1, 117.3, 115.0, 72.5, 61.7, 28.2, 27.9. Anal. Calcd for C₁₂H₁₄F₃NO₂: C, 55.17; H, 5.40; N, 5.36. Found: C, 55.22; H, 5.50; N, 5.30.

(*S*)-1-Amino-2-methyl-1-phenylpropan-2-ol (6b). Adapted from published procedure.²⁵ The trifluoroamide **6a** (1.672 g, 6.400 mmol) was heated to reflux in 5% methanolic NaOH solution (15 mL) for 6 h. The reaction mixture was then cooled to room temperature and concentrated. The light yellow solid crude product was dissolved in CH₂Cl₂ (15 mL) and partitioned with H₂O (15 mL), and the aqueous phase was extracted with CH₂Cl₂ (5 \times 15 mL). The combined organic extracts were washed with brine (15 mL), and the aqueous phase was back-extracted with CH₂Cl₂ (2 \times 15 mL). The organic phases were combined, dried over MgSO₄, filtered, and concentrated under reduced pressure to give a pale yellow oil. The crude product was then purified by recrystallization from hexanes–Et₂O, rinsed with hexanes, and dried in vacuo to afford the pure amino alcohol **6b** as a white crystalline solid (0.770 g, 4.66 mmol, 73% yield). ¹H NMR (500 MHz, CDCl₃) δ 7.34–7.27 (m, 5 H), 3.82 (s, 1 H), 2.03 (br s, 3 H), 1.23 (s, 3 H), 1.05 (s, 3 H); ¹³C NMR (125.6 MHz, CDCl₃) δ 142.7, 128.3, 128.0, 127.5, 72.4, 64.7, 27.8, 25.0. Anal. Calcd for C₁₀H₁₃NO: C, 72.69; H, 9.15; N, 8.48. Found: C, 72.52; H, 9.24; N, 8.45.

2,2'-Methylenebis[(4*S*)-5,5-dimethyl-4-phenyl-2-oxazoline] (6). Adapted from published procedure.²⁶ To a solution of amino alcohol **6b** (0.501 g, 3.03 mmol) in CH₂Cl₂ (15 mL) under N₂ was added diethyl malonimide·2HCl²⁷ (0.356 g, 1.54 mmol). The resulting solution was stirred at room temperature for 5 days. The reaction mixture was diluted with H₂O (10 mL). The mixture was extracted with CH₂Cl₂ (5 \times 10 mL). The combined organic layers were washed with brine (15 mL), dried over MgSO₄, filtered, and concentrated. The resulting colorless sticky oily residue was next purified by Kugelrohr distillation (150 °C/0.035 mmHg) to afford the pure bis(oxazoline) **6** as a pale yellow sticky oil, which solidified while drying under high vacuum (0.365 g, 1.01 mmol, 65% yield). ¹H NMR (500 MHz, CDCl₃) δ 7.33–7.26 (m, 10 H), 4.91 (s, 2 H), 3.54 (s, 2 H), 1.60 (s, 6 H), 0.88 (s, 6 H); ¹³C NMR (125.6 MHz, CDCl₃) δ 162.3, 138.8, 128.3, 127.6, 127.3, 88.2, 78.2, 29.8, 29.2, 23.9. HRMS-EI (*m/z*): [M⁺] calcd for C₂₃H₂₆N₂O₂, 362.1989; found, 362.1980.

(*E*)-4,4'-Di-*tert*-butylstilbene (7a).²⁸ To a stirring solution of tricyclohexylphosphine[1,3-bis(2,4,6-trimethylphenyl)-4,5-dihydroimidazole-2-ylidene][benzylidene]ruthenium(IV) dichloride²⁹ (0.17 g, 0.20 mmol, 2 mol %) in CH₂Cl₂ (10 mL) under N₂, freshly distilled (40 °C/0.035 mmHg) 4-*tert*-butylstyrene (1.90 mL, 10.4 mmol) was added via syringe. The reaction mixture was refluxed for 8 h and then filtered through a short silica gel column, being eluted first by hexanes then by hexanes:EtOAc = 18:1. The fractions containing the product were collected and concentrated under reduced pressure. The crude product was recrystallized from boiling methanol (~200 mL), rinsed with methanol, and dried in vacuo to afford the pure **7a** as a white crystalline solid (1.13 g, 3.86 mmol, 74% yield). ¹H NMR (500 MHz, CDCl₃) δ 7.48 (d, 9 Hz, 4 H), 7.40 (d, 9 Hz, 4 H), 7.09 (s, 2 H), 1.36 (s, 18 H);

(22) Pangborn, A. B.; Giardello, M. A.; Grubbs, R. H.; Rosen, R. K.; Timmers, F. J. *Organometallics* **1996**, *15*, 1518–1520.

(23) (a) Schuetz, S. A.; Day, V. W.; Sommer, R. D.; Rheingold, A. L.; Belot, J. A. *Inorg. Chem.* **2001**, *40*, 5292–5295. (b) Bradely, D. C.; Ghotra, J. S.; Hart, F. A. *J. Chem. Soc., Chem. Commun.* **1973**, 1021–1023.

(24) Hitchcock, P. B.; Lappert, M. F.; Smith, R. G.; Barlett, R. A.; Power, P. P. *J. Chem. Soc., Chem. Commun.* **1988**, 1007–1009.

(25) Denmark, S. E.; Stavenger, R. A.; Faucher, A.-M.; Edwards, J. P. *J. Org. Chem.* **1997**, *62*, 3375–3389.

(26) (a) Denmark, S. E.; Stiff, C. M. *J. Org. Chem.* **2000**, *65*, 5875–5878. (b) Müller, D.; Umbrecht, G.; Weber, B.; Pfaltz, A. *Helv. Chim. Acta* **1991**, *74*, 232–240.

(27) Hall, J.; Lehn, J.-M.; DeCian, A.; Fischer, J. *Helv. Chim. Acta* **1991**, *74*, 1–6.

(28) Yang, D.; Wong, M.-K.; Yip, Y.-C.; Wang, X.-C.; Tang, M.-W.; Zheng, J.-H.; Cheung, K.-K. *J. Am. Chem. Soc.* **1998**, *120*, 5943–5952.

(29) (a) For preparation, see: Scholl, M.; Ding, S.; Lee, C. W.; Grubbs, R. H. *Org. Lett.* **1999**, *1*, 953–956. (b) Also commercially available from Strem Chemicals, Inc. (c) For an example of cross metathesis, see: Chatterjee, A. K.; Sanders, D. P.; Grubbs, R. H. *Org. Lett.* **2002**, *4*, 1939–1942.

^{13}C NMR (125.6 MHz, CDCl_3) δ 150.8, 135.0, 127.9, 126.4, 125.8, 34.8, 31.5. Anal. Calcd for $\text{C}_{22}\text{H}_{28}$: C, 90.35; H, 9.65. Found: C, 90.11; H, 9.70.

(1R,2R)-1,2-Di(4-*tert*-butylphenyl)ethane-1,2-diol (7b). Adapted from published procedure.³⁰ A 250 mL round-bottomed Morton-type flask equipped with a magnetic stirrer was charged with 18.2 g of AD-mix- β , 38.3 mg of $\text{K}_2\text{OsO}_2(\text{OH})_4$, 405.1 mg of $(\text{DHQD})_2\text{PHAL}$, 65 mL of *tert*-butyl alcohol, and 65 mL of water. Stirring at room temperature produced two clear phases; the lower aqueous phase appears bright yellow. Methanesulfonamide (1.24 g, 13.0 mmol) was then added at this point, and the mixture was cooled to 0 °C, whereupon some of the dissolved salts precipitated. (*E*)-4,4'-Di-*tert*-butylstilbene (**7a**) was added all at once, and the heterogeneous slurry was stirred vigorously at 0 °C for 1 day. While the mixture was stirring at 0 °C, solid sodium sulfite (19.5 g) was added, the mixture was allowed to warm to room temperature, and was then stirred for an additional 30 min. Ethyl acetate (130 mL) was next added to the reaction mixture, and after separation of the layers, the aqueous phase was further extracted with EtOAc (3 \times 65 mL). The combined organic layers were washed with 2 N KOH (2 \times 100 mL), dried over MgSO_4 , and concentrated to give the diol and the ligand as a light yellow oil, which solidified upon standing. This crude product was purified by flash chromatography on silica gel (hexanes:EtOAc = 5:1 to 4:1) to give the pure, enantioenriched (>99% ee) diol **7b** as a white solid (4.18 g, 12.8 mmol, 98% yield). Racemic **7b**, used as a standard for chiral HPLC analysis, was synthesized by the identical method except for using 5 mol % DABCO (1,4-diazabicyclo[2.2.2]octane) instead of $(\text{DHQD})_2\text{PHAL}$.³¹ ^1H NMR (400 MHz, CDCl_3) δ 7.31 (d, 8 Hz, 4 H), 7.17 (d, 8 Hz, 4 H), 4.76 (s, 2 H), 2.71 (s, 2 H), 1.31 (s, 18 H); ^{13}C NMR (100.6 MHz, CDCl_3) δ 150.8, 137.3, 126.5, 125.2, 78.4, 34.8, 31.6. Anal. Calcd for $\text{C}_{22}\text{H}_{30}\text{O}_2$: C, 80.94; H, 9.26. Found: C, 81.04; H, 9.43.

(1R,2S)-2-Azido-1,2-di(4-*tert*-butylphenyl)ethan-1-ol (7c). Adapted from published procedure.³² (A) To a cooled, magnetically stirred solution of diol **7b** (1.02 g, 3.12 mmol) and triethylamine (1.74 mL, 12.5 mmol) in CH_2Cl_2 (10 mL) under N_2 , thionyl chloride (0.34 mL, 4.7 mmol) was added dropwise. After the solution was stirred for 15 min at 0 °C, TLC (hexanes:Et₂O = 4:1) revealed complete consumption of the starting diol **7b**. The reaction mixture was next diluted with cold ether (50 mL) and washed with cold water (2 \times 15 mL) and brine (15 mL). The organic solution was dried over MgSO_4 , filtered, and concentrated in vacuo to afford the crude cyclic sulfite, which was used in the next step without further purification. (B) A mixture of the crude cyclic sulfite from the previous step and NaN_3 (0.46 g, 7.1 mmol) in anhydrous DMF (15 mL) was stirred under N_2 for 12 h at 100 °C. Next, the mixture was diluted with Et₂O (150 mL), washed with water (3 \times 15 mL) and brine (15 mL), dried over MgSO_4 , filtered, and concentrated. Purification of the crude product by flash column chromatography on silica gel (hexanes:Et₂O = 9:1 then 4:1) afforded the pure azido alcohol **7c** as a white crystalline solid (1.00 g, 2.85 mmol, 91% isolated yield). ^1H NMR (400 MHz, CDCl_3) δ 7.43 (d, 8.4 Hz, 2 H), 7.41 (d, 8 Hz, 2 H), 7.32 (d, 8.4 Hz, 2 H), 7.30 (d, 8 Hz, 2 H), 4.76 (d, 7.6 Hz, 1 H), 4.62 (d, 7.6 Hz, 1 H), 1.95 (br s, 1 H), 1.35 (s, 18 H); ^{13}C NMR (100.6 MHz, CDCl_3) δ 151.8, 151.4, 137.2, 133.5, 127.8, 126.9, 125.9, 125.4, 76.9, 71.2, 35.0, 34.9, 31.7, 31.6. Anal. Calcd for $\text{C}_{22}\text{H}_{29}\text{N}_3\text{O}$: C, 75.18; H, 8.32; N, 11.96. Found: C, 74.93; H, 8.39; N, 11.82.

(1R,2S)-2-Amino-1,2-di(4-*tert*-butylphenyl)ethan-1-ol (7d). To a stirred suspension of LiAlH_4 (376 mg, 9.90 mmol) in THF (75 mL) at

0 °C under N_2 was slowly added azide **7c** (2.32 g, 6.60 mmol). The resulting green reaction mixture was allowed to warm to room temperature over a period of 3 h. Next, the dark gray suspension was diluted with THF (75 mL) and then carefully quenched by sequential additions of water (0.4 mL), 15% aqueous NaOH (0.4 mL), and water (1.2 mL). Stirring at room temperature for a further 30 min yielded a clear solution and a white precipitate, which was removed by filtration. The filtrate was dried over Na_2SO_4 , filtered, and concentrated under reduced pressure. The crude white product was purified by recrystallization from ~40 mL of hot boiling toluene to afford 2.14 g (6.57 mmol, 99% isolated yield) of amino alcohol **7d** as a white crystalline solid. ^1H NMR (500 MHz, CDCl_3) δ 7.37 (d, 8.5 Hz, 4 H), 7.30 (t, 8.5 Hz, 4 H), 4.62 (d, 7.5 Hz, 1 H), 4.07 (d, 7.5 Hz, 1 H), 1.66 (br s, 3 H), 1.34 (s, 18 H); ^{13}C NMR (125.6 MHz, CDCl_3) δ 151.1, 150.8, 139.2, 138.3, 127.5, 127.0, 125.6, 125.4, 78.9, 62.0, 34.74, 34.71, 31.6. Anal. Calcd for $\text{C}_{22}\text{H}_{31}\text{NO}$: C, 81.18; H, 9.60; N, 4.30. Found: C, 81.13; H, 9.63; N, 4.43.

2,2'-Methylenebis[(4S,5R)-4,5-di(4-*tert*-butylphenyl)-2-oxazoline] (7). Using a procedure similar to that used for synthesizing **6** (vide supra), compound **7** was obtained in 31% yield (108 mg, 0.158 mmol, white solid) from amino alcohol **7d** (332 mg, 1.02 mmol) after recrystallization from Et₂O, followed by rinsing with pentane. ^1H NMR (500 MHz, CDCl_3) δ 7.00 (d, 8.0 Hz, 4 H), 6.96 (d, 8.0 Hz, 4 H), 6.92 (d, 8.0 Hz, 4 H), 6.88 (d, 8.0 Hz, 4 H), 3.89 (s, 2 H), 1.16 (s, 18 H), 1.13 (s, 18 H); ^{13}C NMR (100.6 MHz, CDCl_3) δ 163.3, 150.4, 149.9, 134.7, 133.5, 127.6, 126.4, 124.4, 86.4, 74.1, 34.5, 34.4, 31.43, 31.40. HRMS-EI (m/z): [M^+] calcd for $\text{C}_{47}\text{H}_{58}\text{N}_2\text{O}_2$, 682.4493; found, 682.4479.

(1R,2S)-2-Azido-1,2-di(1-naphthyl)ethan-1-ol (8c). Using the same procedure as used for synthesizing **7c** (vide supra), compound **8c** was obtained in 90% yield (1.21 g, 3.59 mmol, orange oil) from compound **8b** (purchased from Aldrich, 1.25 g, 3.97 mmol). ^1H NMR (400 MHz, CDCl_3) δ 8.00–7.80 (m, 6 H), 7.61–7.58 (m, 2 H), 7.52–7.39 (m, 6 H), 5.96 (d, 6.4 Hz, 1 H), 5.86 (d, 6.4 Hz, 1 H), 2.28 (s, 1 H); ^{13}C NMR (125.6 MHz, CDCl_3) δ 135.9, 134.0, 133.8, 132.0, 131.8, 131.4, 129.5, 129.1, 126.7, 126.4, 126.0, 125.7, 125.4, 123.0, 73.4, 67.4. Anal. Calcd for $\text{C}_{22}\text{H}_{17}\text{N}_3\text{O}$: C, 77.86; H, 5.05; N, 12.38. Found: C, 77.59; H, 4.99; N, 12.11.

(1R,2S)-2-Amino-1,2-di(1-naphthyl)ethan-1-ol (8d). Using the same procedure as used for synthesizing **7d** (vide supra), compound **8d** was obtained in 65% yield (white solid, 560 mg, 1.79 mmol) from compound **8c** (939 mg, 2.77 mmol) after recrystallization from Et₂O and rinsing with hexanes. ^1H NMR (400 MHz, CDCl_3) δ 8.00 (m, 1 H), 7.89 (d, 9 Hz, 1 H), 7.83 (t, 7 Hz, 2 H), 7.74 (d, 8 Hz, 2 H), 7.54 (dd, 10 Hz, 7 Hz, 2 H), 7.44 (quartet, 7 Hz, 2 H), 7.38–7.29 (m, 4 H), 5.86 (d, 6 Hz, 1 H), 5.39 (d, 6 Hz, 1 H), 1.85 (br s, 3 H); ^{13}C NMR (100.6 MHz, CDCl_3) δ 137.8, 136.7, 133.7, 133.6, 132.1, 131.6, 128.9, 128.8, 128.4, 128.2, 126.1, 125.9, 125.6, 125.5, 125.4, 125.2, 124.9, 124.4, 123.4, 123.1, 74.9. HRMS-Cl (m/z): [MH^+] calcd for $\text{C}_{22}\text{H}_{19}\text{NO}$, 314.1539; found, 314.1541.

2,2'-Methylenebis[(4S,5R)-4,5-di(1-naphthyl)-2-oxazoline] (8). Using a procedure similar to that used for synthesizing **6** (vide supra), compound **8** was obtained in 46% yield (white solid, 150 mg, 0.228 mmol) from amino alcohol **8d** (309 mg, 0.985 mmol) after recrystallization from benzene–hexanes followed by rinsing with hexanes. ^1H NMR (400 MHz, CDCl_3) δ 7.98 (d, 8 Hz, 2 H), 7.84 (d, 8 Hz, 2 H), 7.52–6.95 (m, 26 H), 6.74 (d, 10 Hz, 2 H), 4.19 (s, 2 H); ^{13}C NMR (100.6 MHz, CDCl_3) δ 132.9, 131.6, 130.1, 128.2, 128.0, 127.6, 126.3, 125.6, 125.2, 125.0, 124.8, 124.7, 124.4, 123.3, 122.9, 82.9, 69.7. HRMS-EI (m/z): [M^+] calcd for $\text{C}_{47}\text{H}_{34}\text{N}_2\text{O}_2$, 658.2615; found, 658.2607.

{2,2'-Methylenebis[(4S)-4-*tert*-butyl-2-oxazolinato]}Lu[CH(TMS)]₂ (10). A solution of 2,2'-methylenebis[(4S)-4-*tert*-butyl-2-oxazoline] (**2**; 0.25 g, 0.93 mmol) in toluene (20 mL) was added slowly under inert atmosphere to a solution of $\text{Lu}[\text{CH}(\text{TMS})_2]_3$ (0.60 g, 0.92 mmol) in toluene (50 mL) at –78 °C. The mixture was allowed to

- (30) (a) Bennani, Y. L.; Sharpless, K. B. *Tetrahedron Lett.* **1993**, *34*, 2079–2082. (b) Sharpless, K. B.; Amberg, W.; Bennani, Y. L.; Crispino, G. A.; Hartung, J.; Jeong, K.-S.; Kwong, H.-L.; Morikawa, K.; Wang, Z.-M.; Xu, D.; Zhang, X.-L. *J. Org. Chem.* **1992**, *57*, 2768–2771.
(31) Bandini, M.; Cozzi, P. G.; Gazzano, M.; Umani-Ronchi, A. *Eur. J. Org. Chem.* **2001**, 1937–1942.
(32) (a) Review of cyclic sulfites: Lohray, B. B. *Synthesis* **1992**, 1035–1052. (b) Lohray, B. B.; Ahuja, J. R. *J. Chem. Soc., Chem. Commun.* **1991**, 95–97. (c) Kim, B. M.; Sharpless, K. B. *Tetrahedron Lett.* **1990**, *31*, 4317–4320.

warm to room temperature and was then stirred for 2 h. Volatiles were removed in vacuo and the resulting white solid was extracted with pentane (25 mL). The filtrate was next concentrated to 2 mL. Cooling at $-30\text{ }^{\circ}\text{C}$ for 20 h afforded colorless crystals. A second crop of crystals was obtained from the mother liquor. Combined yield: 480 mg (69% yield). ^1H NMR (400 MHz, C_6D_6) δ 4.65 (s, 1 H), 4.00 (dd, 8 Hz, 4 H, 2 H), 3.78–3.73 (m, 4 H), 0.89 (s, 18 H), 0.37 (s, 18 H), 0.31 (s, 18 H), -0.95 (s, 2 H). ^{13}C NMR (100.6 MHz, C_6D_6) 175.7, 74.06, 68.90, 60.08, 51.72, 35.19, 26.77, 6.69, 1.79. Anal. Calcd for $\text{C}_{29}\text{H}_{63}\text{N}_2\text{O}_2\text{Si}_4\text{Lu}$: C, 45.88; H, 8.36; N, 3.69. Found: C, 45.42; H, 8.32; N, 3.49.

2,2-Diphenyl-4-pentenitrile (13a). A flame-dried 500 mL Schlenk flask was charged with *n*-BuLi (65 mL of a 1.6 M solution in hexanes, 104 mmol) and THF (100 mL) at $-78\text{ }^{\circ}\text{C}$ under N_2 . To the resulting light yellow solution was slowly added distilled diisopropylamine (14.6 mL 104 mmol) via syringe, and the mixture was stirred at $-78\text{ }^{\circ}\text{C}$ for 30 min. Next, diphenylacetonitrile (18.93 g, 98.0 mmol) was added at $-78\text{ }^{\circ}\text{C}$, and the reaction mixture was warmed to $0\text{ }^{\circ}\text{C}$. Stirring at $0\text{ }^{\circ}\text{C}$ for 1 h produced an intense yellow solution. Allyl bromide (8.65 mL, 100 mmol) was then added all at once by syringe, and the reaction mixture was allowed to warm to room temperature and stirred for 3 h. The reaction was next quenched by addition of water (100 mL), and the resulting phases were separated. The aqueous layer was then extracted with Et_2O ($4 \times 100\text{ mL}$). The combined organic layers were washed with water (100 mL), saturated aqueous NH_4Cl solution ($2 \times 100\text{ mL}$), and brine (100 mL) and were then dried over MgSO_4 , filtered, and concentrated to give a yellow oily crude product. Purification by flash column chromatography on silica gel (hexanes: $\text{Et}_2\text{O} = 12:1$) afforded pure pentenenitrile **13a** (22.5 g, 96.4 mmol, 98% yield). ^1H NMR (400 MHz, CDCl_3) δ 7.45–7.30 (m, 10 H), 5.82–5.72 (m, 1 H), 5.26 (d, 18 Hz, 1 H), 5.22 (d, 10 Hz, 1 H), 3.19 (d, 7.6 Hz, 2 H); ^{13}C NMR (100.6 MHz, CDCl_3) δ 139.7, 131.8, 128.8, 127.9, 127.0, 122.0, 120.4, 51.9, 44.1. HRMS- EI (m/z): [M^+] calcd for $\text{C}_{17}\text{H}_{15}\text{N}$, 233.1199; found, 233.1193. Anal. Calcd for $\text{C}_{17}\text{H}_{15}\text{N}$: C, 87.52; H, 6.48; N, 6.00. Found: C, 87.85; H, 6.70; N, 6.21.

2,2-Diphenyl-4-penten-1-amine (13). To a stirred suspension of LiAlH_4 (1.63 g, 43.0 mmol) in Et_2O (75 mL) at $0\text{ }^{\circ}\text{C}$ under N_2 was slowly added a solution of nitrile **13a** (7.71 g, 33.1 mmol) in Et_2O (25 mL). The reaction mixture was allowed to warm to room temperature and stirred at room temperature for 5 h. Next, the mixture was diluted with Et_2O (75 mL) and then carefully quenched by sequential additions of water (1.63 mL), 15% aqueous NaOH (1.63 mL), and water (5.0 mL). Stirring at room temperature for a further 30 min yielded a colorless solution with a white precipitate, which was then removed by filtration. The filtrate was dried over Na_2SO_4 , filtered, and concentrated under reduced pressure. The crude amine was purified by Kugelrohr distillation ($140\text{ }^{\circ}\text{C}/0.04\text{ mmHg}$) to afford 7.37 g (31.1 mmol, 94% isolated yield) of pure amine **13** as a clear, colorless oil. ^1H NMR (500 MHz, CDCl_3) δ 7.32–7.29 (m, 4 H), 7.23–7.19 (m, 6 H), 5.46–5.37 (m, 1 H), 5.07 (d, 17 Hz, 1 H), 4.99 (d, 11 Hz, 1 H), 3.34 (s, 2 H), 2.94 (d, 6 Hz, 2 H), 0.84 (br s, 2 H); ^{13}C NMR (125.6 MHz, CDCl_3) δ 146.4, 134.8, 128.4, 128.3, 126.2, 117.9, 51.5, 48.7, 41.3. HRMS- CI (m/z): [MH^+] calcd for $\text{C}_{17}\text{H}_{20}\text{N}$, 238.1590; found, 238.1588. Anal. Calcd for $\text{C}_{17}\text{H}_{20}\text{N}$: C, 86.03; H, 8.07; N, 5.90. Found: C, 85.98; H, 7.88; N, 5.98.

X-ray Crystallographic Study of [(4S)-BuBox]Lu[CH(TMS)₂]₂ (10). A suitable crystal of **10** was mounted using Paratone-N oil (Exxon) on a glass fiber and positioned in a Bruker SMART-1000 CCD diffractometer. Crystal data collection parameters are summarized in Table 1. Data were processed using SAINT-NT from Bruker, and all calculations were performed using the Bruker SHELXTL³³ crystallographic software package. Cell reduction calculations on all data showed **10** to crystallize in the orthorhombic space group $P2_12_12_1$.³⁴

Table 1. X-ray Diffraction Data Collection Parameters for **10**

empirical formula	$\text{C}_{29}\text{H}_{63}\text{N}_2\text{O}_2\text{Si}_4\text{Lu}$
formula weight	759.14
crystal size, mm^3	$0.227 \times 0.060 \times 0.249$
crystal color, habit	colorless, plate
crystal system	orthorhombic
space group	$P2_12_12_1$
<i>a</i> , Å	11.7693(9)
<i>b</i> , Å	17.6598(14)
<i>c</i> , Å	18.4591(15)
α , deg	90
β , deg	90
γ , deg	90
Volume, Å ³	3836.6(5)
<i>Z</i>	4
<i>d</i> (calcd), g cm^{-3}	1.314
diffractometer	Bruker SMART-1000CCD
temperature	$-120\text{ }^{\circ}\text{C}$
<i>m</i>	27.23 cm^{-1}
radiation	graphite-monochromated Mo K α
λ	0.710 73 Å
exposure time	20 s
scan width	0.30°
2θ range, deg	$1.6\text{--}28.3$
intensities (unique, <i>R_i</i>)	34 867 (9213, 0.0442)
<i>R</i>	0.0286
<i>R_w</i> ²	0.0588
no. of parameters	343
goodness-of-fit on <i>F</i> ²	0.954
min, max density in ΔF map	$-0.63, 1.96\text{ e}^{-}/\text{\AA}^{-3}$

Intensity data were corrected for Lorentz, polarization, and anomalous dispersion effects.³⁴ The structure was solved by direct methods³⁵ and expanded using Fourier techniques.³⁶ The non-hydrogen atoms were refined anisotropically. Hydrogen atoms were included but not refined. The final cycle of full-matrix least-squares refinement on *F*² was based on 9213 reflections and 343 variable parameters and converged (largest parameter shift was 0.002 times its esd) with unweighted and weighted agreement factors of *R* = 0.0286, *R_w*² = 0.0588.

Typical NMR-Scale Catalytic Reactions. In the glovebox, the lanthanide catalyst precursor $\text{Ln}[\text{N}(\text{TMS})_2]_3$ (7.2 μmol) and neutral BoxH ligand (8.7 μmol) were weighed into an NMR tube equipped with a Teflon valve (J-Young), and a solution of the internal NMR integration standard (*p*- $\text{CH}_3\text{C}_6\text{H}_4$)₄Si in C_6D_6 (35 mM, 200 μL , 7 μmol) was added by syringe. The mixture was next further diluted with C_6D_6 (300 μL). The tube was then removed from the glovebox and shaken by hand to yield a homogeneous, clear solution. The ensuing *in situ* generation of the (Box) $\text{Ln}[\text{N}(\text{TMS})_2]_2$ precatalyst was monitored by ^1H NMR, and the complete consumption of the starting $\text{Ln}[\text{N}(\text{TMS})_2]_3$ complex was observed within 2 h. Next, the tube was attached to the high vacuum line. On the vacuum line, the tube was evacuated while the benzene solution was frozen at $-78\text{ }^{\circ}\text{C}$. The substrate (ca. 1 M in C_6D_6 , 0.15 mL, 20-fold molar excess) was added via syringe under an Ar flush. The tube was next evacuated and backfilled with Ar 3 times while frozen at $-78\text{ }^{\circ}\text{C}$. The tube was then sealed, thawed, and brought to the desired temperature, and the ensuing hydroamination reaction was monitored by ^1H NMR. After the reaction was complete, the reaction mixture was freeze–thaw degassed and the volatiles were vacuum-transferred into a separate NMR tube. The solvent was removed on a rotary evaporator at $0\text{ }^{\circ}\text{C}$ to give the product. Alternatively, for nonvolatile products, filtration of the reaction mixture through a small plug of silica gel removes the catalyst. The silica gel was rinsed with Et_2O (5 mL); the fractions were combined and evaporated under reduced pressure to afford the product.

2-Methyl-4,4-diphenylpyrrolidine (14). ^1H NMR (500 MHz, CDCl_3) δ 7.35–7.28 (m, 8 H), 7.21–7.19 (m, 2H), 3.71 (d, 11 Hz, 1 H), 3.51 (d, 11 Hz, 1 H), 3.44–3.37 (m, 1 H), 2.78 (dd, 13 Hz, 6.5 Hz,

(33) *SHELXTL for WindowsNT: Crystal Structure Analysis Package*; Bruker: 1997.

(34) Cromer, D. T.; Waber, J. T. *International Tables for X-ray Crystallography*; The Kynoch Press: Birmingham, England, 1974; Vol IV.

(35) Sheldrick, G. M. *SHELXS-97*; 1990.

(36) Sheldrick, G. M. *SHELXL-97*; 1997.

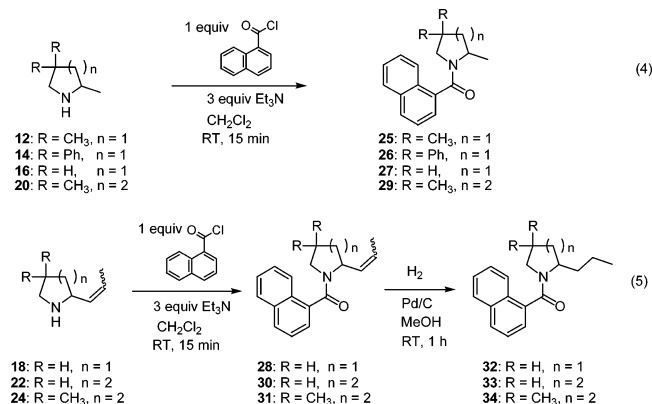
Table 2. Chiral Stationary Phase HPLC Conditions for Determination of Enantiomeric Excess

Entry	Compound ^a	Column	Eluent ratio hexane:PrOH	Flow rate mL / min	Retention time (absolute config)
1.		(S,S)-Whelk-O1	90 : 10	1.0	6.2 min (1 <i>R</i> ,2 <i>R</i>) 10.2 min (1 <i>S</i> ,2 <i>S</i>)
2.		(S,S)-Whelk-O1	98 : 02	1.0	6.5 min (1 <i>R</i> ,2 <i>S</i>) 7.7 min (1 <i>S</i> ,2 <i>R</i>)
3.		(<i>R,R</i>)-β-Gem1	75 : 25	1.0	9.4 min (<i>S</i>) 16.9 min (<i>R</i>)
4.		(<i>S,S</i>)-Whelk-O1	80 : 20	2.0	8.5 min (<i>R</i>) 46.5 min (<i>S</i>)
5.		(<i>R,R</i>)-β-Gem1	75 : 25	1.0	11.5 min (<i>S</i>) 23.0 min (<i>R</i>)
6.		(<i>S,S</i>)-Whelk-O1	80 : 20	1.5	24.8 min (<i>R</i>) 43.4 min (<i>S</i>)
7.		(<i>S,S</i>)-Whelk-O1	75 : 25	1.5	12.9 min (<i>R</i>) 26.4 min (<i>S</i>)
8.		(<i>S,S</i>)-Whelk-O1	75 : 25	1.5	8.6 min (<i>R</i>) 36.9 min (<i>S</i>)
9.		(<i>S,S</i>)-Whelk-O1	80 : 20	2.0	12.8 min (<i>R</i>) 31.4 min (<i>S</i>)
10.		(<i>R,R</i>)-β-Gem1	85 : 15	1.5	9.4 min (<i>S</i>) 16.7 min (<i>R</i>)

^a Ar = 4-*tert*-butylphenyl; R = 1-naphthoyl.

1 H), 2.07 (dd, 13 Hz, 9 Hz, 1 H), 1.24 (d, 6.5 Hz, 3 H); ¹³C NMR (125.6 MHz, CDCl₃) δ 147.99, 147.28, 128.47, 128.44, 127.21, 127.14, 126.14, 126.11, 58.09, 57.47, 53.23, 47.25, 22.59. HRMS-EI (*m/z*): [M⁺] calcd for C₁₇H₁₉N, 237.1512; found, 237.1510.

Determination of Enantiomeric Excess and Absolute Configuration. The values for enantiomeric excess of chiral products were determined by chiral stationary phase HPLC analysis using a Regis (*S,S*)-Whelk O1 column (i.d. = 4.6 mm, length = 250 mm, particle size = 5 mm) or a Regis (*R,R*)-β-Gem1 column (i.d. = 4.6 mm, length = 250 mm, particle size = 5 mm).³⁷ The HPLC conditions are listed in Table 2. The 2-substituted azacycle hydroamination products in Table 7 were derivatized as 1-naphthoyl amides for HPLC analysis by treating with 1-naphthoyl chloride and Et₃N in CH₂Cl₂ (eqs 4 and 5).^{37c} Racemic



standard samples were prepared by the hydroamination/cyclization of corresponding amine substrates with achiral lanthanide catalysts such

as Cp²LnCH(TMS)₂ or Ln[N(TMS)₂]₃. In case of aminodiene hydroamination/cyclizations producing *E/Z* olefin mixture products, the product mixtures were derivatized similarly and then hydrogenated to afford the corresponding 2-propyl substituted azacycle naphthylamides (eq 5).³⁸ Absolute configurations were determined by optical rotation (Table 2, entries 3, 4, 6, 8, and 9),^{8,10a} or tentatively assigned from comparison of the elution order of HPLC experiments with those of similar compounds (Table 2, entries 5, 7, and 10),³⁹ or based on the Sharpless' mnemonic scheme (Table 2, entries 1 and 2).³⁰

Kinetic Studies of Hydroamination/Cyclization. In a typical experiment, an NMR sample was prepared as described above (see Typical NMR-Scale Catalytic Reactions) but maintained at −78 °C until kinetic measurements were begun. For experiments in which the catalyst concentration was varied, a stock solution of precatalyst (a total 3.00 mL C₆D₆ solution of La[N(TMS)₂]₃ (123.6 mg) and (4*R*,5*S*)-Ph₂BoxH (**5**, 112.4 mg), 66.4 mM based on quantitative formation) was prepared and sequentially diluted to five different concentrations with C₆D₆ and frozen at −78 °C until the substrates were added. After substrate addition, the sample tube was inserted into the probe of the INOVA-500 spectrometer which had been previously set to the desired temperature (*T* ± 0.2 °C; checked with a methanol or ethylene glycol temperature standard). A single acquisition (nt = 1) with a 45° pulse was used during data acquisition to avoid saturation. The reaction kinetics were usually monitored from intensity changes in one of the olefinic resonances over three or more half-lives. The substrate concentration was measured from the olefinic peak area, A_s, standardized to A_i, the methyl peak area of the (*p*-CH₃C₆H₄)₄Si internal standard. Typically, data collected up to two half-lives could be convincingly fit by least-squares to eq 6 where [substrate]₀ is the initial concentration of substrate ([substrate]₀ = A_{s0}/A_{i0}). The turnover frequency, *N_t* (h^{−1}), was calculated from the least-squares determined slope (*m*) according to eq 7 where [catalyst]₀ is the initial concentration of the precatalyst.

$$[\text{substrate}] = mt + [\text{substrate}]_0 \quad (6)$$

$$N_t (\text{h}^{-1}) = -(60 \text{ min h}^{-1}) * m / [\text{catalyst}]_0 \quad (7)$$

Results and Discussion

The goal of this study was to develop configurationally stable C₂-symmetric bis(oxazolinato)lanthanide catalysts for intramolecular enantioselective hydroamination/cyclization. This section first presents synthetic routes to the variously substituted bis(oxazoline) ligands. Next, in situ protonolytic generation of bis(oxazolinato)lanthanide catalysts and the X-ray crystal structure of one of these catalysts are discussed. Systematic optimization of these in situ generated catalysts with regard to catalytic enantioselective hydroamination/cyclization is then described, including effects of lanthanide ion, ligand:Ln stoichiometry, and ligand architectures on catalytic rates and enantioselectivity, as well as kinetic studies suggesting mechanistic scenarios and catalyst molecularities. Finally, results of enantioselective aminoalkene and aminodiene hydroamination/cyclizations medi-

(37) For examples of separation of racemates using an (*S,S*)-Whelk-O1 column, see: (a) Pirkle, W. H.; Welch, C. J. *Tetrahedron: Asymmetry* **1994**, 5, 777–780. (b) Pirkle, W. H.; Welch, C. J.; Lamm, B. *J. Org. Chem.* **1992**, 57, 3854–3860. For an example of separation of 2-substituted piperidines, see: (c) Hyun, M. H.; Jin, J. S.; Lee, W. *Bull. Korean Chem. Soc.* **1997**, 18, 336–339.

(38) Reverse order (hydrogenation then derivatization) also produced the same results.

(39) Elution orders of 1-naphthoyl amide derivatives of 2-methylpyrrolidine, 2-methylpiperidine, 2-ethoxycarbonylpyrrolidine, and 2-ethoxycarbonylpiperidine on an (*S,S*)-Whelk-O1 column were established in terms of their absolute configuration, and the second eluted enantiomers were assigned as *S* (*R* in case of ethoxycarbonyl due to Cahn–Ingold–Prelog priority change).^{37c} Compound **25**, **27**, **29**, **30**, and **33** also showed the identical trend.

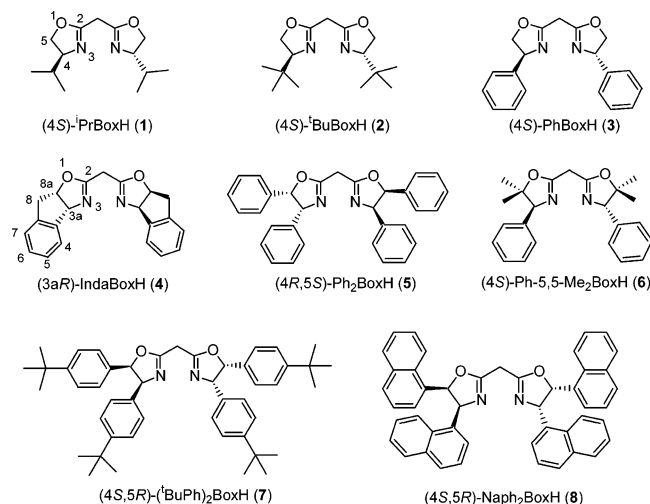
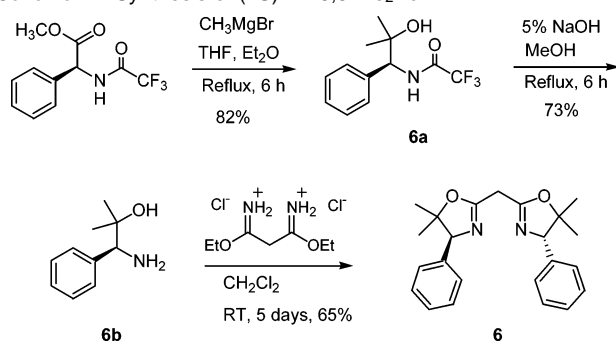


Figure 1. Bis(oxazoline) ligands screened.

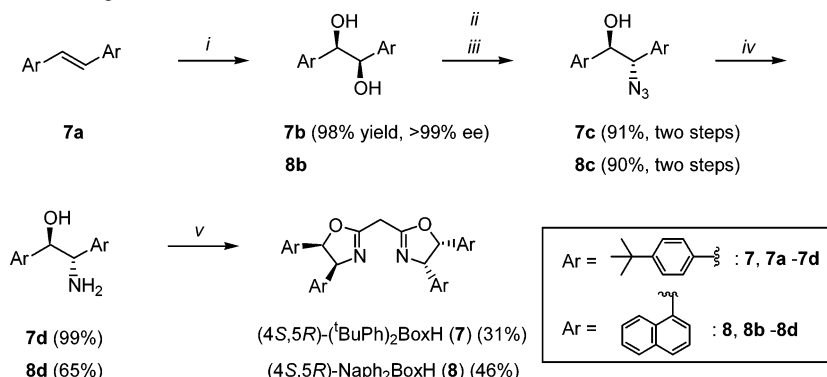
Scheme 2. Synthesis of (4S)-Ph-5,5-Me₂BoxH



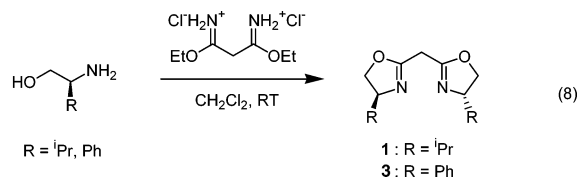
ated by the optimized catalytic systems are presented and compared with previous results using chiral organolanthanocenes, followed by a discussion of plausible stereochemical pathways.

Ligand Synthesis. Figure 1 shows a list of the bis(oxazoline) ligands examined in this study. Compounds **2**, **4**, and **5** are commercially available, and compounds **1** and **3** were synthesized from the corresponding amino alcohols according to published procedures (eq 8).²⁶ To explore the effects of the bis(oxazoline) ligand substitution pattern on lanthanide complex reactivity and selectivity, several new bis(oxazoline) ligands were also synthesized. Compound **6** with *gem*-dimethyl substitution on the 5 position was synthesized by adapting published

Scheme 3. Synthesis of Ar₂BoxH Ligands^a

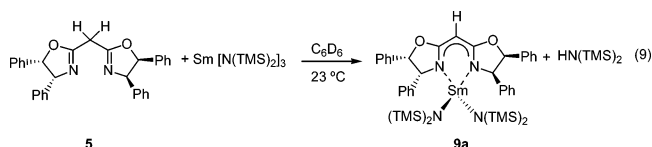


^a Reagents and conditions: (i) 1 mol% K₂OsO₂(OH)₄, 5 mol% (DHQD)₂PHAL, 3 equiv of K₃Fe(CN)₆, 3 equiv of K₂CO₃, 1 equiv of CH₃SO₂NH₂, ^tBuOH–H₂O (1:1), 0 °C, 1 day; (ii) SOCl₂, Et₃N, CH₂Cl₂, 0 °C, 15 min; (iii) NaN₃, DMF, 100 °C, 12 h; (iv) LiAlH₄, THF, 0 °C to rt, 3 h; (v) diethylmalonimidate–2HCl, CH₂Cl₂, rt, 5 days.



procedures, as described in Scheme 2.²⁵ Addition of methylmagnesium bromide to the commercially available *N*-trifluoroacetyl-protected (*S*)-2-phenylglycine methyl ester, followed by deprotection and condensation with malonimidate,²⁷ affords ligand **6** in good yield. A general synthetic scheme for diaryl substituted ligands **7** and **8** is summarized in Scheme 3. Thus, Sharpless asymmetric dihydroxylation^{30,40} of 4,4'-di(*tert*-butyl)-stilbene (**7a**) affords diol **7b** in excellent ee (>99%) and isolated yield (98%). The C₂-symmetric diol **7b** was then treated with thionyl chloride to form a cyclic sulfite, which was subsequently opened by the azide nucleophile with complete inversion of the stereogenic center.³² Lithium aluminum hydride reduction of azide **7c** produces amino alcohol **7d** in excellent yield. However, condensation of **7d** with malonimidate proceeds very slowly to afford bis(oxazoline) ligand **7** in modest yield (31%), and about 50% of starting amino alcohol **7d** is recovered from the reaction mixture. Dinaphthyl substituted bis(oxazoline) ligand **8** was similarly synthesized from the commercially available diol **8b**.

In Situ Generation of Precatalysts. To initially probe the feasibility of an amine elimination route to bis(oxazolino)-lanthanide complexes, reaction of the homoleptic lanthanide amide²³ Sm[N(TMS)₂]₃ with neutral bis(oxazoline) ligand **5** was monitored by ¹H NMR (eq 9). A key event in this reaction is



the protonolysis of one of the bulky bistrimethylsilyl amido ligands by the relatively acidic methylene protons of the bis(oxazoline) compound. As illustrated in Figure 2, the paramagnetically shifted ¹H resonance of the starting Sm[N(TMS)₂]₃ (δ –1.6 ppm) disappears in ~1 h (~95% consumed), while the resonances of byproduct HN(TMS)₂ (δ 0.1 ppm) and one major product (δ –2.0 ppm) appear cleanly. Based on integration of those resonances and X-ray crystal structures of related bis-

Table 3. Selected Bond Distances (Å) and Angles (deg) for (4*S*)-^tBuBoxLu[CH(TMS)₂]₂ (**10**)

bond distances					
Lu	N1A	2.259(3)	O4A	C3A	1.424(6)
Lu	N11A	2.255(3)	C3A	C2A	1.537(6)
Lu	C1	2.362(4)	N11A	C7A	1.321(5)
Lu	C8	2.356(4)	N11A	C10A	1.484(5)
N1A	C5A	1.336(5)	C6A	C7A	1.377(6)
N1A	C2A	1.504(5)	O8A	C7A	1.359(5)
C5A	C6A	1.390(6)	O8A	C9A	1.432(6)
O4A	C5A	1.345(5)	C9A	C10A	1.535(6)
bond angles					
N11A–Lu–N1A	85.24(12)	C7A–C6A–C5A	125.1(4)		
C1–Lu–C8	120.03(16)	C7A–N11A–Lu1	124.0(3)		
C5A–N1A–Lu1	120.9(3)	C10A–N11A–Lu1	126.6(2)		
C2A–N1A–Lu1	131.4(3)	C7A–N11A–C10A	109.0(3)		
C5A–N1A–C2A	105.4(3)	N11A–C7A–C6A	129.7(4)		
N1A–C5A–C6A	129.7(4)				

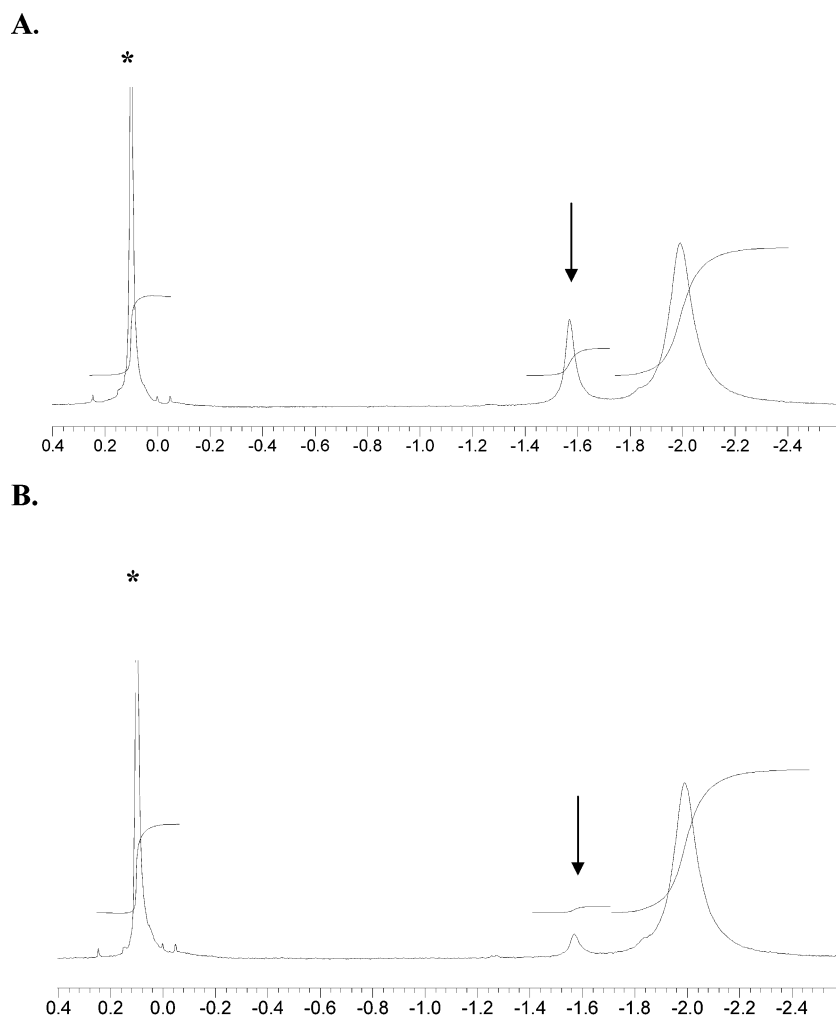
(oxazolinato)lanthanide complexes, the structure of the major product is proposed to be a pseudo-tetrahedral lanthanide(III) complex with one bis(oxazoline) ligand and two bistrimethylsilylamido ligands (**9a**), as depicted in eq 9. Although time for the in situ generation varies slightly (15 min–2 h at 23 °C) with the bis(oxazoline) ligand structure, the amine elimination reactions of homoleptic lanthanide amides with 1.2 equiv of

Table 4. Effect of Varying Lanthanide Metal Center and Ligand Equivalents on Turnover Frequencies and Enantiomeric Excess in Intramolecular Hydroamination/Cyclization

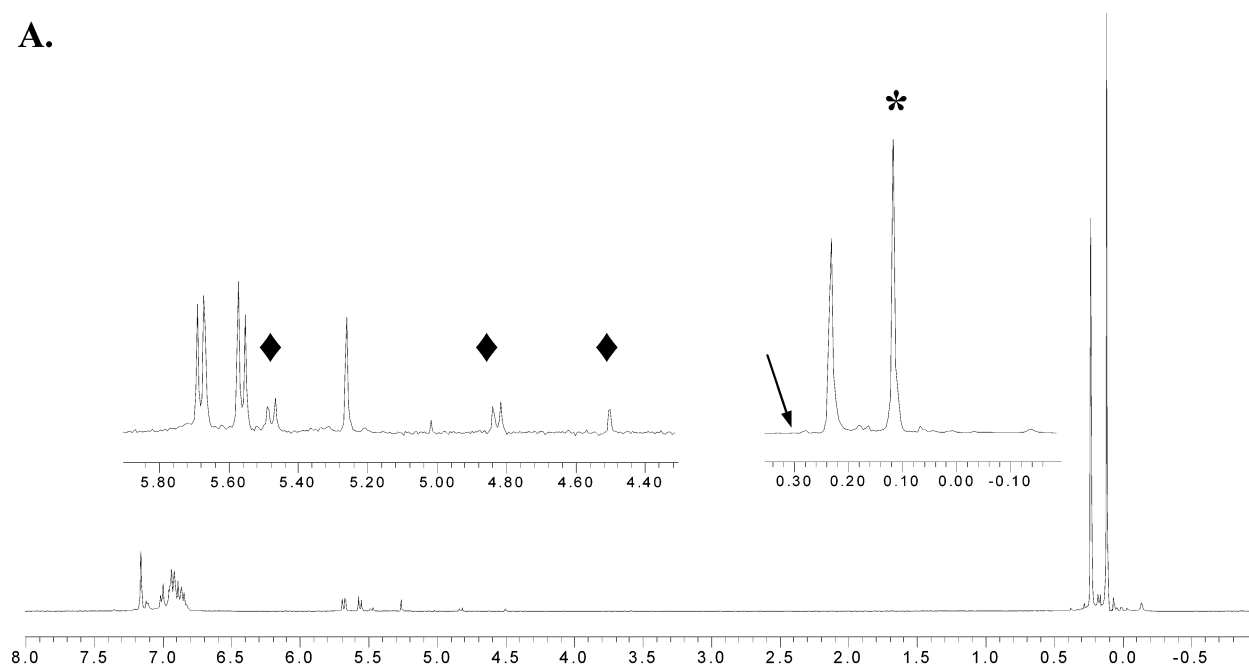
entry	Ln	BoxH/Ln[N(TMS) ₂] ₃	temp (°C)	N _t ^a (h ^{−1})	% ee ^b (config.) ^c
1	Sm	0	23	5.2 ^d	control expt
2	Sm	1.2	23	13	55 (<i>R</i>)
3	Sm	2.3	60		60 (<i>R</i>)
4	Nd	1.2	23	~10	61 (<i>R</i>)
5	La	0	23	7.7 ^d	control expt
6	La	1.2	23	25	67 (<i>R</i>)
7	La	2.3	23	10	63 (<i>R</i>)

^a *N_t* calculated from two half-lives. ^b Enantiomeric excess determined by chiral HPLC analysis. ^c A (−) optical rotation correlates to the *R* configuration for these pyrrolidines and piperidines. See ref 8. ^d Initial *N_t* estimated from one half-life due to the first-order-like kinetics in [substrate].

various bis(oxazoline) ligands (**1–8**) proceed equally well under the typical hydroamination reaction conditions ([Ln] = ~10 mM, C₆D₆). In all cases, the starting homoleptic lanthanide

**Figure 2.** In situ ¹H NMR monitoring of the reaction of Sm[N(TMS)₂]₃ with 1.2 equiv of bis(oxazoline) **5** in benzene-*d*₆ at 23 °C: (A) after 15 min; (B) after 55 min. The arrows indicate the resonances of the starting homoleptic amide, Sm[N(TMS)₂]₃, and the asterisks indicate resonances of the byproduct HN(TMS)₂.

A.



B.

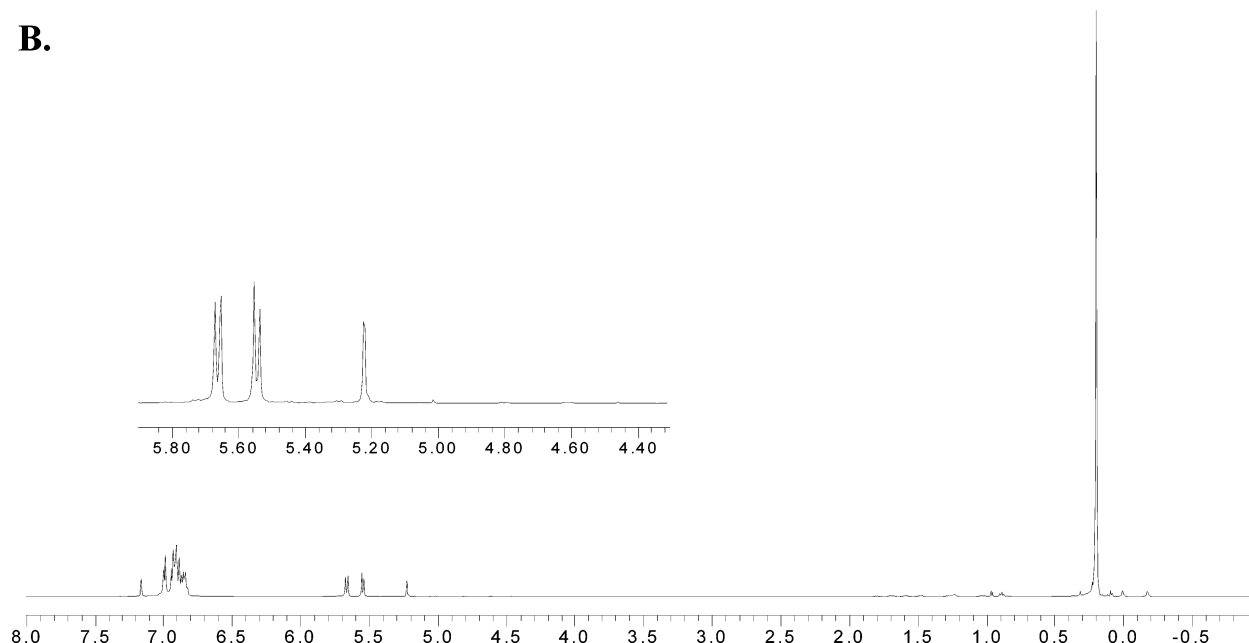


Figure 3. (A) ^1H NMR spectrum of the crude reaction mixture of $\text{La}[\text{N}(\text{TMS})_2]_3$ with 1.2 equiv of bis(oxazoline) **5** in benzene- d_6 at 23 °C after 1 h. The arrow indicates the resonance of the starting $\text{La}[\text{N}(\text{TMS})_2]_3$, the asterisk indicates the resonance of the byproduct $\text{HN}(\text{TMS})_2$, and the diamonds are tentatively assigned to resonances of a $[(4R,5S)\text{-Ph}_2\text{Box}]_2\text{La}[\text{N}(\text{TMS})_2]$ byproduct. (B) ^1H NMR spectrum of the isolated $[(4R,5S)\text{-Ph}_2\text{Box}]\text{La}[\text{N}(\text{TMS})_2]_2$ in benzene- d_6 .

amide $\text{Ln}[\text{N}(\text{TMS})_2]_3$ is consumed ($\geq 94\%$ by ^1H NMR), the resulting reaction mixture remains a clear, homogeneous solution, and the resulting crude NMR shows predominantly one major product $(\text{Box})\text{Ln}[\text{N}(\text{TMS})_2]_2$ and the byproduct $\text{HN}(\text{TMS})_2$. Figure 3A illustrates another example of the in situ generation process. With a more open La^{3+} metal center, the starting homoleptic $\text{La}[\text{N}(\text{TMS})_2]_3$ (δ 0.28 ppm, singlet) peak disappears within 15 min. Compared to the ^1H NMR spectrum of the isolated $[(4R,5S)\text{-Ph}_2\text{Box}]\text{La}[\text{N}(\text{TMS})_2]_2$ complex (**9b**; Figure 3B),⁴¹ the ^1H NMR of an in situ generated reaction mixture (Figure 3A) principally exhibits $[(4R,5S)\text{-Ph}_2\text{Box}]\text{La}[\text{N}(\text{TMS})_2]_2$ and $\text{HN}(\text{TMS})_2$ along with small quantities of what is tentatively assigned to $[(4R,5S)\text{-Ph}_2\text{Box}]_2\text{La}[\text{N}(\text{TMS})_2]$.⁴²

Attempts to obtain diffraction-quality single crystals of any of the aryl-substituted box complexes have so far been unsuccessful. The sterically bulky secondary amine byproduct $\text{HN}(\text{TMS})_2$ is expected to be a poor ligand and is unlikely to compete with either hydroamination substrates or product amines for coordination at lanthanide centers. Thus, the in situ generation method described here provides a very convenient route to

(40) For a recent review of Sharpless asymmetric dihydroxylation, see: (a) Johnson, R. A.; Sharpless, K. B. In *Catalytic Asymmetric Synthesis*, 2nd ed.; Ojima, I., Ed.; VCH: New York, 2000; pp 357–398. (b) Bolm, C.; Hildebrand, J. P.; Muniz, K. In *Catalytic Asymmetric Synthesis*, 2nd ed.; Ojima, I., Ed.; VCH: New York, 2000; pp 399–428. (c) Markó, I. E.; Svendsen, J. S. In *Comprehensive Asymmetric Catalysis*; Springer: Jacobsen, E. N., Pfaltz, A., Yamamoto, H., Eds.; Berlin, 1999; Vol. II, pp 714–787.

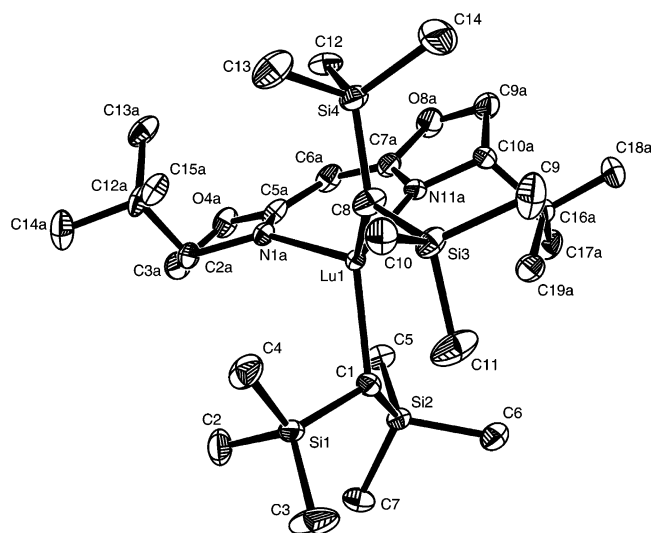
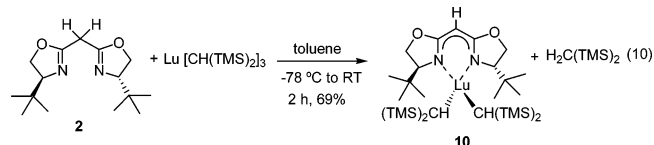


Figure 4. Molecular structure of [(4*S*)-'BuBox]Lu[CH(TMS)₂]₂ (**10**). Thermal ellipsoids are drawn at the 30% probability level.

libraries of chiral lanthanide precatalysts for enantioselective hydroamination.

Molecular Structure of the Precatalyst, [(4*S*)-'BuBox]-Lu[CH(TMS)₂]₂ (10**).** The proposed structure of the present bis-(oxazolinato)lanthanide complexes is further supported by the X-ray crystal structure of [(4*S*)-'BuBox]Lu[CH(TMS)₂]₂, synthesized via an analogous alkane elimination route (eq 10).



Single crystals of **10** suitable for X-ray diffraction were grown from a concentrated pentane solution at $-30\text{ }^{\circ}\text{C}$, and the molecular structure is shown in Figure 4 with pertinent bond lengths and angles compiled in Table 3. A C_2 -symmetry axis exists at the Lu⁺³ center, which is coordinated in a distorted tetrahedral fashion. The bis(trimethylsilyl)methyl ligands in **10** are oriented away from the *tert*-butyl groups of the C_2 -symmetric 'BuBox fragment, minimizing nonbonded interactions. It appears that the bis(oxazolinato) negative charge is extensively delocalized, suggested by the elongated N1A–C5A distance (1.336(5) Å) and the shortened C5A–C6A distance (1.390(6) Å). The Lu1–N1A and Lu1–N11A distances are identical (2.259(3) Å and 2.255(3) Å, respectively). Lu1–C5A, Lu1–C6A, and Lu1–C7A distances are significantly longer (3.161(4) Å, 3.559(4) Å, and 3.187(4) Å, respectively) than Lu–CH(TMS)₂ bond distances (Lu1–C1 = 2.362(4) Å and Lu1–C8 = 2.356(4) Å).

(41) Preparative scale synthesis of [(4*R*,5*S*)-Ph₂Box]La[N(TMS)₂]₂ (**9b**): Onto a mixture of La[N(TMS)₂]₃ (307 mg, 0.495 mmol) and 2,2'-methylenebis-[(4*R*,5*S*)-4,5-diphenyl-2-oxazoline] (**5**) (245 mg, 0.534 mmol) was vacuum transferred toluene (20 mL) at $-78\text{ }^{\circ}\text{C}$. The mixture was allowed to warm to room temperature and was then stirred for 5 h to yield a pale-yellow clear solution. The solvent was removed in vacuo, and hexanes (60 mL) were then vacuum transferred onto the residue. After stirring for 30 min at room temperature, the solvent was removed in vacuo to yield a off-white powder (384 mg, 0.419 mmol, 85%). ¹H NMR (500 MHz, C₆D₆): δ 7.00–6.84 (m, 20 H), 5.67 (d, 8.0 Hz, 2 H), 5.54 (d, 8.0 Hz, 2 H), 5.22 (s, 1 H), 0.20 (s, 36 H). ¹³C NMR (100.6 MHz, C₆D₆): 174.7, 139.3, 136.7, 129.0, 128.8, 128.5, 128.3, 128.0, 126.9, 85.1, 72.6, 58.9, 4.4. Anal. Calcd for C₄₃H₆₁N₄O₂Si₄La: C, 56.31; H, 6.70; N, 6.11. Found: C, 57.66; H, 6.42; N, 5.95.

(42) When 2.0 equiv of **5** are added (Table 4, entry 7), the peaks marked with diamonds become the major species.

suggesting a negligible π contribution to the ligand–Lu bonding in this complex. The N1A–Lu1–N11A bite angle of the six-membered chelate formed by the 'BuBox ligand is 85.24(12) $^{\circ}$. The two oxazoline ring planes are twisted relative to one another by 15.7 $^{\circ}$. The structure of [(4*S*)-'BuBox]Y[N(SiHMe₂)₂]₂ reported by Anwander and co-workers exhibits similar metrical parameters when corrections are made for differences in Lu³⁺ and Y³⁺ ionic radii.^{19c}

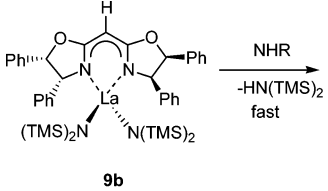
Effects of Metal Ion and Ligand: Ln Stoichiometry on Catalytic Rates and Enantioselectivity. To find the catalytically optimum lanthanide ion and equivalents of bis(oxazoline) ligands with respect to the lanthanide precursor, the standard cyclization **11** \rightarrow **12** was performed using the C_2 -symmetric bis(oxazolinato)lanthanide complexes generated in situ from NMR-scale reactions of 5 mol % Ln[N(TMS)₂]₃ (Ln = La, Nd, Sm) with 6 or 11 mol % (4*R*,5*S*)-Ph₂BoxH ligand (**5**) in C₆D₆ (Table 4). Hydroamination/cyclization **11** \rightarrow **12** was chosen as a standard reaction for evaluation studies because of relatively large observed turnover frequencies (presumably reflecting the *gem*-dimethyl substitution, the Thorpe–Ingold effect)⁴³ and the abundance of comparative data with many previously investigated C_1 -symmetric catalysts.⁸ Since initial screening experiments with isolated bis(oxazolinato)Lu bisalkyl complex **10** revealed sluggish rates and very low enantioselectivities (<15%) for intramolecular hydroamination/cyclizations, including **11** \rightarrow **12**, lanthanides with larger ionic radii (La, Nd, Sm) typically exhibiting higher N_t 's for the aminoalkene hydroamination/cyclization were chosen. In addition, for the lanthanide reagent, triamides (Ln[N(TMS)₂]₃)²³ were chosen over trialalkyls (Ln[CH(TMS)₂]₃)²⁴ because of more convenient synthetic routes and superior thermal stability, especially for lanthanides having larger ionic radii (La, Nd, Sm). Results in Table 4 show that both maximum N_t (25 h^{−1} at 23 $^{\circ}\text{C}$) and ee (67%) values are obtained with La[N(TMS)₂]₃ + 1.2 equiv of ligand **5** (entry 6).⁴⁴ Interestingly, % ee also increases with metal ionic radius (55% (Sm) < 61% (Nd) < 67% (La); Table 4, entries 2, 4, and 6, respectively), in contrast to the results with C_1 -symmetric, Cp-based chiral catalysts, where enantioselectivity maximizes at Y or Sm.⁸ Note that the use of ligand **5** also maximizes the reaction rate (Table 4, entries 2 and 6 vs entries 1 and 5, respectively), implying that chiral ligand **5** stabilizes the catalytically active species and minimizes possible contributions from nonstereoselective background reactions mediated by La-[NHR]₃.^{13d} Interestingly, use of 2.3 equiv of ligand:Ln precursor depresses turnover frequencies but has little effect on enantioselectivity (Table 4, entries 3 and 7). Therefore, La[N(TMS)₂]₃ + 1.2 equiv of bis(oxazoline) ligand was employed for further studies.

Kinetic Studies. Quantitative kinetic studies of the standard cyclization **11** \rightarrow **12** were carried out by in situ ¹H NMR spectroscopic monitoring. The [(4*R*,5*S*)-Ph₂Box]La[N(TMS)₂]₂ catalyst (**9b**) was generated in situ and used without isolation (see the Experimental Section). Since all La–N(TMS)₂ groups may not undergo immediate protonolysis, tetra(*p*-tolyl)silane

(43) (a) Eliel, E. L.; Wilen, S. H. *Stereochemistry of Organic Compounds*; John Wiley & Sons: New York, 1994; pp 682–684. (b) Kirby, A. J. *Adv. Phys. Org. Chem.* **1980**, *17*, 183–278.

(44) When isolated [(4*R*,5*S*)-Ph₂Box]La[N(TMS)₂]₂ was employed as a precatalyst, slightly higher N_t (35 h^{−1}) and similar ee (64% ee) values were observed for the **11** \rightarrow **12** reaction compared to the result with the in situ generated precatalyst (N_t = 25 h^{−1}, 67% ee, Table 4, entry 6).

Table 5. Ratio of Two Plausible Catalytically Active Bis(oxazolinato)lanthanide Complexes as a Function of Initial [Substrate]/[Precatalyst] Ratio

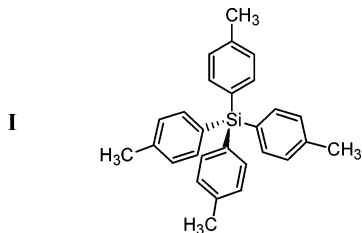


9b

J

[substrate]/[precatalyst]	J:K
9	47:53
13	42:58
18	35:65
35	25:75
83	17:83

(**I**)⁴⁵ was employed as an internal NMR integration standard rather than HN(TMS)₂. The methyl signal of **I** (δ 2.1 ppm) has



a very short T₁ [1.25 (\pm 0.05) s in C₆D₆ at 23 °C] and appreciable intensity. Moreover, it can be distinguished from the substrate **11**, product **12**, and various catalyst signals at 500 MHz. The cyclizations were performed with a 10–90-fold molar excess of substrate, and in all cases, substrate was completely consumed. The decrease of an olefinic (δ 5.0 ppm) resonance was monitored as a function of time and normalized versus internal standard **I**.

The precatalyst [(4*R*,5*S*)-Ph₂Box]La[N(TMS)₂]₂ (**9b**) is rapidly activated upon addition of amine substrate **11**, with at least one La–N(TMS)₂ group undergoing immediate protonolysis. However, in contrast to La[N(TMS)₂]₃, where all three La–N(TMS)₂ groups are cleaved upon substrate addition,⁴⁶ it appears by ¹H NMR that the cleavage of the second La–N(TMS)₂ group of [(4*R*,5*S*)-Ph₂Box]La[N(TMS)₂]₂ does not proceed to completion, presumably reaching an equilibrium mixture depending on the [substrate]/[precatalyst] ratio and identity of bis(oxazoline) ligand (Table 5). The J:K ratio can be estimated from integration of the resonances of free HN(TMS)₂ (δ 0.12 ppm) and bound La–N(TMS)₂ in complex **J** (δ 0.23 ppm), assuming a rapid and complete **9b** \rightarrow **J** step. Higher [substrate]/

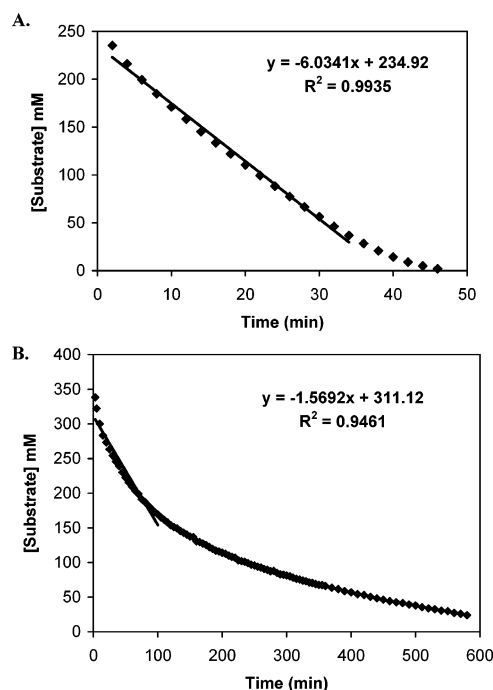


Figure 5. (A) Substrate concentration as a function of time for the hydroamination/cyclization of 2,2-dimethyl-4-penten-1-amine (**11**) in benzene-*d*₆ at 23 °C using the precatalyst [(4*R*,5*S*)-Ph₂Box]La[N(TMS)₂]₂ generated in situ from La[N(TMS)₂]₃ and (4*R*,5*S*)-Ph₂BoxH (**5**). The line is the least-squares fit to the data points up to three half-lives. (B) Substrate concentration as a function of time for the hydroamination/cyclization of 2,2-dimethyl-4-penten-1-amine (**11**) in benzene-*d*₆ at 23 °C using the precatalyst La[N(TMS)₂]₃. The line is the least-squares fit to the data points up to one half-life.

[precatalyst] ratios generate slightly more **K** species, suggesting the second protonolysis to be slow relative to the cyclization of **11**.

Figure 5A presents kinetic data typical of many runs, which reveal the rate of hydroamination/cyclization to be zero-order in [substrate] over at least three half-lives. In contrast, the kinetic data for a control experiment, La[N(TMS)₂]₃ (without added **5**)-mediated hydroamination/cyclization, show a first-order-like exponential plot (Figure 5B). Since some quantities of white precipitate form after approximately one half-life in the latter control experiment, that this first-order-like behavior may be a consequence of catalyst deactivation rather than a true mechanistic change cannot be rigorously excluded.

A plot of the reaction rate versus precatalyst concentration for the **11** \rightarrow **12** cyclization mediated by in situ generated [(4*R*,5*S*)-Ph₂Box]La[N(TMS)₂]₂ (**9b**), in which substrate concentration is held constant and precatalyst concentration is varied over an \sim 10-fold range, shows the reaction to be first order in catalyst concentration (Figure 6). Thus, the empirical rate law (eq 11) is essentially the same as was observed for hydroamination/cyclization by lanthanocenes

$$\text{Rate} = k[\text{substrate}]^0[\text{catalyst}]^1 \quad (11)$$

such as Cp²LnCH(TMS)₂, Me₂Si(Cp²)(Cp^{*})LnE(TMS)₂ or Me₂Si(OHF)(Cp^{*})LnE(TMS)₂.^{8,10b,13i,14c,15b} Despite the differences in the number of substrate amido ligands at the Ln³⁺ center (BoxLn = 2 vs Cp²Ln = 1) and presence of two potential catalysts, BoxLn(NHR)[N(TMS)₂] and BoxLn(NHR)₂, the same mechanism appears to be operative, including turnover-limiting

(45) For an example of using (*p*-tolyl)₄Si as an internal NMR integration standard, see: Stahl, N. G.; Zuccaccia, C.; Jensen, T. R.; Marks, T. J. *J. Am. Chem. Soc.* **2003**, *125*, 5256–5257.

(46) The ¹H NMR integration ratio of [HN(TMS)₂]:[internal standard] remains constant throughout the reaction, and no other Ln–N(TMS)₂ signals are observed in the ¹H NMR.

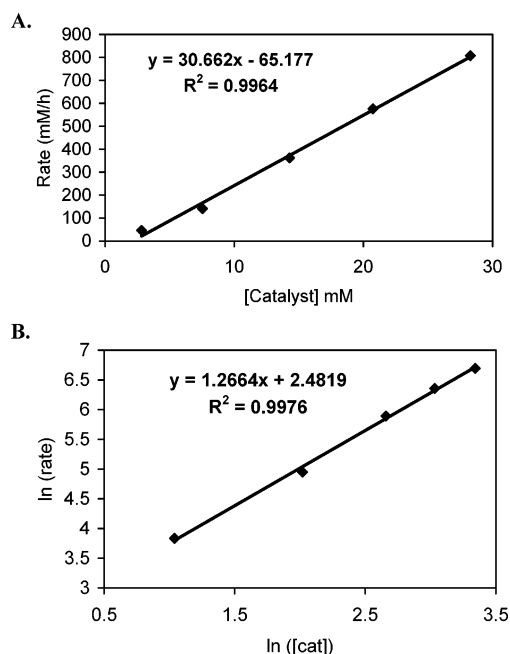


Figure 6. (A) Determination of reaction order in lanthanide concentration for the hydroamination/cyclization of 2,2-dimethyl-4-penten-1-amine (**11**) in benzene-*d*₆ at 23 °C using the precatalyst [(4*R*,5*S*)-Ph₂Box]La[N(TMS)₂]₂ generated in situ from La[N(TMS)₂]₃ and (4*R*,5*S*)-Ph₂BoxH (**5**). (B) van't Hoff plot for the hydroamination/cyclization of 2,2-dimethyl-4-penten-1-amine (**11**) in benzene-*d*₆ at 23 °C using the precatalyst [(4*R*,5*S*)-Ph₂Box]-La[N(TMS)₂]₂ generated in situ from La[N(TMS)₂]₃ and (4*R*,5*S*)-Ph₂BoxH (**5**). The lines are least-squares fits to the data points.

Table 6. Bis(oxazoline) Ligand Survey in Enantioselective Hydroamination/Cyclization

entry	ligand	<i>N</i> _t ^a (h ⁻¹)	% ee ^b (config.) ^c
1	(4 <i>S</i>)- ^{<i>i</i>} PrBoxH (1)	3.2	6 (<i>R</i>)
2	(4 <i>S</i>)- ^{<i>t</i>} BuBoxH (2)	1.3	39 (<i>R</i>)
3	(4 <i>S</i>)-PhBoxH (3)	7.1	56 (<i>S</i>)
4	(3 <i>aR</i>)-IndaBoxH (4)	1.8	25 (<i>R</i>)
5	(4 <i>R</i> ,5 <i>S</i>)-Ph ₂ BoxH (5)	25	67 (<i>R</i>)
6	(4 <i>S</i>)-Ph-5,5-Me ₂ BoxH (6)	21	61 (<i>S</i>)
7	(4 <i>S</i> ,5 <i>R</i>)-(^{<i>t</i>} BuPh) ₂ BoxH (7)	17	55 (<i>S</i>)
8	(4 <i>S</i> ,5 <i>R</i>)-Naph ₂ BoxH (8)	17	59 (<i>S</i>)

^a *N*_t calculated from two half-lives. ^b Enantiomeric excess determined by chiral HPLC analysis. ^c A (–) optical rotation correlates to the *R* configuration for these pyrrolidines and piperidines. See ref 8.

olefin insertion into the Ln–N bond followed by rapid amine protonolysis of the resulting Ln–C linkage (Scheme 1). Furthermore, that the rate is first order in [catalyst] also strongly suggests monomeric catalytically active species or at least species with relatively static molecularity for the bis(oxazolinato)lanthanide-catalyzed hydroamination.

Ligand Survey. To optimize Box ligand structures for enantioselective hydroamination/cyclization, a number of variously substituted bis(oxazoline) ligands were screened in the model cyclization of **11** (Table 6). Results for 4-substituted bis(oxazoline) ligands (**1**, **2**, and **3**) demonstrate that phenyl stereodirecting groups lead to both higher selectivities (56% ee) and turnover frequencies (7.1 h⁻¹) than alkyl groups such as

^{*i*}Pr and ^{*t*}Bu (6% ee/ 3.2 h⁻¹ and 39% ee/1.3 h⁻¹, respectively; Table 6, entries 1–3). Interestingly, the absolute configurations of the products observed with arylBoxH ligands, **3**–**8**, are opposite to those observed with alkylBoxH ligands **1** and **2** (Table 6, entries 3–8 vs entries 1–2).⁴⁷ Note that substitutions at the 5 position of PhBoxH appear to be crucial for higher selectivity and turnover frequency. Also, both product enantiomeric excess and cyclization turnover frequencies are further increased by 5,5-*gem*-dimethyl substitution (61% ee, 21 h⁻¹; Table 6, entry 6) or an additional phenyl substitution at the 5 position (67% ee, 25 h⁻¹; Table 6, entry 5). However, attempts to further increase ee's by utilizing more sterically demanding aryl groups such as 1-naphthyl or 4-(*tert*-butyl)phenyl (Table 6, entries 7 and 8) were not successful. Nevertheless, the observed enantioselectivity for cyclization of **11** with the in situ generated [(4*R*,5*S*)-Ph₂Box]La[N(TMS)₂]₂ precatalyst (67% ee at 23 °C) is greater than some of the highest ee's previously observed with C₁-symmetric Cp-based chiral organolanthanides. For example, cyclization of **11** at 25 °C proceeds with a maximum 56% ee using the first-generation (*R*)-Me₂Si(Cp'')-(Cp(–)-phenylmenthyl)YCH(TMS)₂ precatalyst^{8b} and with 32% ee using the (*S*)-Me₂Si(OHF)(Cp(–)-menthyl)SmN(TMS)₂ precatalyst.^{8a}

Reaction Scope. Enantioselective hydroamination/cyclization with the in situ generated [(4*R*,5*S*)-Ph₂Box]La[N(TMS)₂]₂ precatalyst (**9b**) was investigated for a range of aminoalkene and aminodiene substrates in forming five- and six-membered heterocycles (Table 7).⁴⁸ In contrast to C₁-symmetric chiral organolanthanocene precatalysts which typically exhibit rather substrate-specific enantioselectivity (Table 8), the current bis(oxazolinato) catalyst system affords more consistent ee's. Thus, cyclization of terminal alkenylamine substrates **11**, **15**, and **17** using the C₂-symmetric [(4*R*,5*S*)-Ph₂Box]La[N(TMS)₂]₂ precatalyst (**9b**) proceeds with 67%, 40%, and 56% ee, respectively (Table 7, entries 1, 3, and 5).⁴⁹ The current result can be compared to the best collection of the previous results at a similar temperature: 56% ee for **11** → **12**, 69% ee for **15** → **16**, and 67% ee for **19** → **20** (Table 8, entries 3, 7, and 15, respectively). Enantiomeric excess values for the cyclization of aminodiene substrates **17**, **21**, and **23** using [(4*R*,5*S*)-Ph₂Box]-La[N(TMS)₂]₂ precatalyst **9b** are 17%, 54%, and 45% ee, respectively (Table 7, entries 4, 6, and 7) and are comparable to or greater than those with C₁-symmetric Cp-based precatalysts at similar reaction temperatures (23–41%, 37–63%, and 19% ee, respectively; Table 8, entries 9–11, 16–17, and 19). The reported enantiomeric excess values of the aminodiene cyclization products in Table 7 were determined by chiral HPLC

- (47) For examples of reversal of product absolute configuration in other metal-bis(oxazoline) complex-mediated asymmetric transformation, see: (a) Evans, D. A.; Masse, C. E.; Wu, J. *Org. Lett.* **2002**, *4*, 3375–3378. (b) Evans, D. A.; Janey, J. M. *Org. Lett.* **2001**, *3*, 2125–2128. (c) Evans, D. A.; Johnson, J. S.; Burgey, C. S.; Campos, K. R. *Tetrahedron Lett.* **1999**, *40*, 2879–2882.
- (48) The in situ generated [(4*R*,5*S*)-Ph₂Box]La[N(TMS)₂]₂ precatalyst (**9b**) was chosen based on the ligand screening result for the reaction **11** → **12**. This assumption is supported by the following results. For the reaction **17** → **18**, La[N(TMS)₂]₃ + ligand **6** affords product **18** (*E*:*Z* = 60:40) with *N*_t = 6.0 h⁻¹ and 7% ee (*R*) at 23 °C, and La[N(TMS)₂]₃ + ligand **8** yields product **18** (*E*:*Z* = 44:56) with *N*_t = 1.7 h⁻¹ and 8% ee (*S*) at 23 °C. For the reaction **19** → **20**, Sm[N(TMS)₂]₃ + ligand **5** proceeds with *N*_t ≈ 2 h⁻¹ and 9% ee (*S*) at 60 °C. However, it cannot be ruled out that the catalyst system (metal precursor and ligand) must be optimized for each substrate.
- (49) Several of the aminohexene cyclizations (entries 5 and 6 in Table 7) are sluggish at 23 °C and require heating to 60 °C to obtain useful turnover frequencies.

Table 7. Reaction Scope in Enantioselective Hydroamination/Cyclization

$\text{H}_2\text{N}-\text{CH}_2-\text{CH}(\text{R})-\text{CH}(\text{R})-\text{CH}_2-\text{CH}=\text{CH}_2 \xrightarrow[\text{C}_6\text{D}_6]{\text{5 mol\% La[N(TMS)}_2\text{]}_3, \text{6 mol\% } \mathbf{5}}$					
Entry	Substrate	Product ^a	<i>N_t</i> (h ⁻¹)	Temp (°C)	%ee ^b (config) ^c
1.			25	23	67 (R)
2.			660 ^d	23	34 (R)
3.			0.09	23	40 (R)
4.			3.0	23	17 (S)
5.			4.0	60	56 (S)
6.			0.6	60	54 (R)
7.			1.4	23	45 (R)

^a Stereochemistry shown for the major enantiomer. ^b Determined by chiral HPLC analysis. ^c Determined by optical rotation (entries 1, 3, and 5) of HCl salt of hydrogenated product (entry 6) and chiral HPLC retention time (entries 2, 4, and 7). ^d 1.3 mol % La[N(TMS)₂]₃ and 1.6 mol % (4*R*,5*S*)-Ph₂BoxH (**5**) used.

analysis of the C=C hydrogenated 1-naphthoyl amides.⁵⁰ However, qualitative HPLC analysis of the 1-naphthoyl amide derivatives of *E/Z* mixtures reveal that the ee of the minor isomer is much different from that of the major product and in some cases the two isomers have opposite signs of optical rotation, lowering the overall observed ee of the hydrogenated product.⁵¹

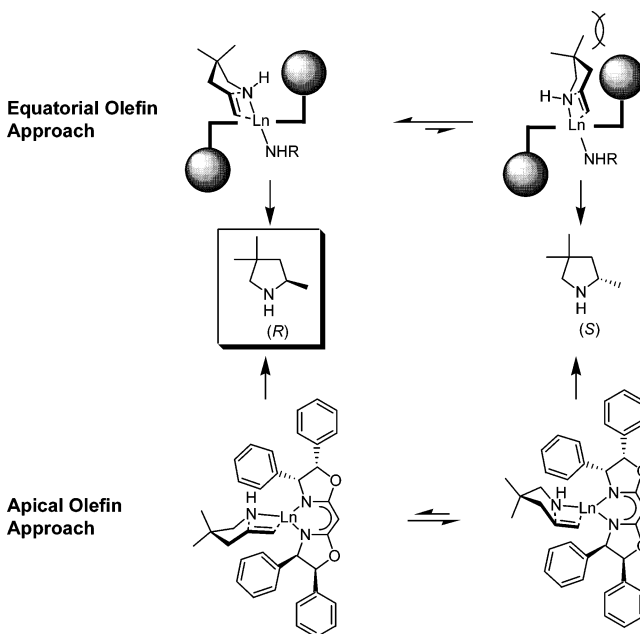
Substrate steric bulk was also varied to investigate the effect on reaction rate and enantioselectivity. Geminal dialkyl substitutions in the carbon backbone of the substrate affect the reaction rates quite significantly (Thorpe–Ingold effect;⁴³ Table 7, entries 1 and 2 vs entry 3 and entry 7 vs entry 6). Compared with previous lanthanocene precatalysts, it appears that the *gem*-dimethyl or *gem*-diphenyl substitution effect is even more pronounced.^{8,13i} However, no obvious correlation is found between the substrate steric bulk and cyclization ee.

Working Model for Enantioselection. The stereochemical pathways of the enantioselective hydroamination/cyclization of aminoalkene **11** can be rationalized by the model shown in Figure 7. The kinetic studies indicate that the in situ generated bis(oxazolinato)lanthanide catalysts follow virtually the same, general organolanthanide-catalyzed hydroamination/cyclization mechanistic scenario established for cyclopentadienyl catalysts, as evidenced by the same rate law and metal ionic radius/substrate structural effects on cyclization rates. Thus, as in the cases of previous C₁-symmetric chiral organolanthanocenes,⁸ nonbonded repulsive interactions are expected to play a significant role in enantioselection during the irreversible,

Table 8. Summary of Previous Hydroamination/Cyclization Results with C₁-Symmetric Chiral Catalysts

$\text{H}_2\text{N}-\text{CH}_2-\text{CH}(\text{R})-\text{CH}(\text{R})-\text{CH}_2-\text{CH}=\text{CH}_2 \longrightarrow \text{Product}$					
Entry	Substrate	Product	Precatalyst ^a	<i>N_t</i> (h ⁻¹)	%ee ^b (config) ^c
1.			(<i>S</i>)-menthylCpSm	84 (25)	53 (S)
2.			(<i>S</i>)-menthylCpSm	- (-30)	74 (S)
3.			(<i>R</i>)-phenylmenthylCpY	8 (25)	56 (S)
4.			(<i>S</i>)-OHFSm	33 (25)	32 (S)
5.			(<i>S</i>)-menthylCpSm	33 (25)	62 (S)
6.			(<i>S</i>)-menthylCpSm	- (0)	72 (S)
7.			(<i>R</i>)-menthylCpY	- (25)	69 (S)
8.			(<i>S</i>)-OHFSm	2.6 (25)	46 (S)
9.			(<i>S</i>)-menthylCpSm	74 (23)	25 (R)
10.			(<i>S</i>)-menthylCpY	0.09 (25)	41 (R)
11.			(<i>S</i>)-OHFSm	12 (25)	23 (R)
12.			(<i>S</i>)-menthylCpSm	2 (25)	15 (R)
13.			(<i>R</i>)-neomenthylCpSm	- (25)	17 (R)
14.			(<i>S</i>)-OHFSm	0.6 (25)	41 (S)
15.			(<i>S</i>)-OHFY	2.1 (25)	67 (S)
16.			(<i>S</i>)-menthylCpSm	0.1 (25)	37 (R)
17.			(<i>S</i>)-OHFSm	0.11 (25)	63 (R)
18.			(<i>S</i>)-OHFSm	- (0)	71 (R)
19.			(<i>S</i>)-OHFSm	1.7 (25)	19 (R)
20.			(<i>S</i>)-OHFSm	- (0)	24 (R)

^a Precatalyst abbreviations: R^{*}CpLn = Me₂Si(CpMe₄)(CpR^{*})LnE(TMS)₂ (R^{*} = (–)-menthyl, (–)-phenylmenthyl, or (+)-neomenthyl; E = CH or N), OHFLn = Me₂Si(η⁵-octahydrofluorenyl)(Cp(–)-menthyl)LnN(TMS)₂. ^b Determined by ¹⁹F NMR or GC-MS analysis of Mosher amides or chiral HPLC analysis of 1-naphthoyl amides. ^c Apparent *R/S* reversals with propenylpyrrolidine (entries 9–11) and propenylpiperidine (entries 16–20) versus methyl azacycles (entries 1–8, 12–15) are simply due to inversion of the Cahn–Ingold–Prelog priority sequence.

**Figure 7.** Stereochemical models for [(4*R*,5*S*)-Ph₂Box]La[N(TMS)₂]₂ catalyzed intramolecular hydroamination/cyclization of 2,2-dimethyl-4-penten-1-amine (**11**). In the drawings representing the apical olefin approach, one amide ligand is omitted for clarity.

turnover-limiting olefin insertion process. Therefore, four reasonable trajectories for insertive olefin approach to the Ln center can be considered by assuming a chairlike seven-membered ring⁵² transition state with the restriction of coplanar

(50) See Experimental Section.

(51) Quantitative analysis was not possible due to the overlap of some peaks.

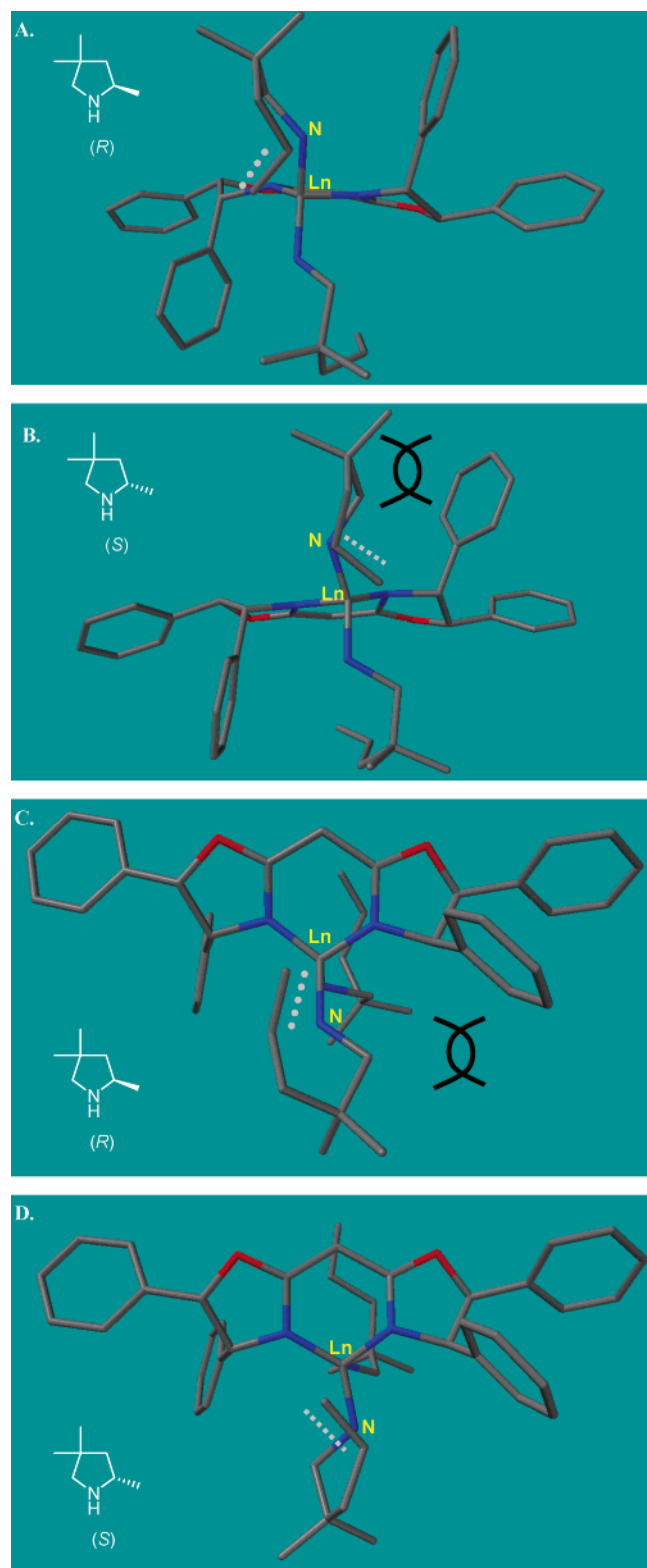


Figure 8. Transition state models for [(4*R*,5*S*)-Ph₂Box]La[N(TMS)₂]₂ catalyzed intramolecular hydroamination/cyclization of 2,2-dimethyl-4-penten-1-amine (**11**). (A) (2*R*)-2,4,4-trimethylpyrrolidine formation via the equatorial approach pathway. (B) (2*S*)-2,4,4-trimethylpyrrolidine formation via the equatorial approach pathway. (C) (2*R*)-2,4,4-trimethylpyrrolidine formation via the apical approach pathway. (D) (2*S*)-2,4,4-trimethylpyrrolidine formation via the apical approach pathway.

Ln, N, and olefinic carbon atoms (Figure 7). In the equatorial approach (similar to “frontal approach” in previous chiral organolanthanocene discussions⁸), the substrate amido group

occupies the apical position and the olefin approaches from the front equatorial site, with the rear equatorial site blocked by the chelating bis(oxazolinato) ligand. In the apical approach (similar to “lateral approach” in previous discussions of chiral organolanthanocenes⁸), the substrate amido group occupies the front equatorial position and the olefin approaches from the top apical position, with another amido ligand presumably present at the bottom apical position. Spartan/MM2-level molecular modeling studies (Figure 8)⁵³ indicate that, in the equatorial approach, the pathway leading to the minor *S* isomer involves unfavorable nonbonded interactions between the carbon chain of the substrate and the ligand stereodirecting (phenyl) groups, whereas, in the apical approach, minor *S* product formation appears to be slightly more favorable than the major *R* isomer formation. Good enantioselectivity (67% ee) with the (4*R*,5*S*)-Ph₂BoxH ligand (**5**), thus, implies that the equatorial approach is favored over the apical approach for the cyclization of substrate **11**. However, in principle, these approaching modes can be controlled by the steric environment of the ligand architecture. In fact, the aforementioned reversal of the product absolute configuration by aryl versus alkyl bis(oxazolinato) ligand substituents may be attributable to a switch in olefin approach, although more sophisticated comparisons can be only made when crystal structures of both alkyl and aryl box lanthanide amide complexes are available. Note also that the current qualitative model ignores any steric effects that may be exerted by labile substrate molecules that may also be present in the coordination sphere.¹³ⁱ

Conclusions

C₂-symmetric bis(oxazolinato)lanthanide complexes catalyze enantioselective intramolecular hydroamination/cyclization of aminoalkenes and aminodienes with good rates and enantioselectivities comparable to or greater than those obtained with C₁-symmetric chiral organolanthanocene catalysts, even for very difficult substrates. The present results represent the rare example of enantioselective hydroamination catalyzed by non-metallocene lanthanide complexes.⁵⁴ These new C₂-symmetric catalyst systems are particularly attractive since they are configurationally stable and can be generated protonolytically

(52) For discussions about the conformations of rings larger than six, see: Eliel, E. L.; Wilen, S. H. *Stereochemistry of Organic Compounds*; John Wiley & Sons: New York, 1994; pp 762–769.

(53) These models were created from the crystal structure of **10** by the following procedure. The mol2 file of the original crystal structure of **10** was loaded into Spartan 2002 Windows program (Wavefunction, Inc., Irvine, 2001). Two *tert*-butyl groups were replaced by phenyl groups, and another two phenyl groups were appended at the 5*R* position of each oxazoline ring. The $-\text{CH}(\text{TMS})_2$ groups were replaced by $-\text{NHCH}_2\text{C}(\text{CH}_3)_2\text{CH}_2\text{CH}=\text{CH}_2$ groups with the Lu–N bond held constant at the crystallographically determined bond length. All bond lengths, bond angles, and dihedral angles around the six-membered chelate were held constant. False Lu–C and N–C bonds were inserted, and the C=C bond was reduced to a C–C bond to form a 4-centered metallacycle, thus mimicking the 4-centered transition state structures for formation of each enantiomer. Next, the molecular energy of the structure was minimized at the MM2 level, and the false bonds were deleted. The calculated images were flipped horizontally in Adobe Photoshop (v. 5.5) to show the mirror image, the (4*R*,5*S*)-Ph₂Box ligand structure.

(54) After this manuscript was submitted, a report of enantioselective aminoalkene hydroamination catalyzed by a chiral lanthanide bisaryloxide complex appeared, which constitutes another example of noncyclopentadienyl lanthanide catalyzed hydroamination.⁹ In this communication, four different ligand structures and three lanthanides (Y, Sm, La) were screened for 2,2-dimethyl-4-penten-1-amine (**11**) cyclization. Up to 61% ee was reported for the La catalyst, although the reaction rate is rather slow ($N_1 \approx 2.5 \text{ h}^{-1}$ at 70 °C, estimated from the reported data; 40 h at 70 °C for 100% conversion using 1 mol % catalyst). This paper also reports decreasing ee with decreasing Ln³⁺ radius.

in situ from commercially available or readily prepared bis-(oxazoline) ligands and the corresponding $\text{Ln}[\text{N}(\text{TMS})_2]_3$ or $\text{Ln}[\text{CH}(\text{TMS})_2]_3$ reagents. The optimized precatalyst, in situ generated $[(4R,5S)\text{-Ph}_2\text{Box}]\text{La}[\text{N}(\text{TMS})_2]_2$ (**9b**), shows more consistent ee values than lanthanocene catalysts over a broad range of substrates including terminal aminoalkenes and aminodienes for five- and six-membered ring formation. Kinetic studies indicate that the rate is in zero order in [amine substrate] and first order in [catalyst]. This and the rate dependence on the Ln^{3+} ionic radius suggest the same mechanism as seen in previous organolanthanide-catalyzed hydroamination/cyclizations and presumably involving monomeric active catalytic species. Guided by the proposed stereochemical model and motivated by the attractive features and promising results of

the present catalyst system, further modification of ligand architecture is currently in progress in our laboratory.

Acknowledgment. Financial support by the NSF (CHE-0078998) is gratefully acknowledged. S.H. thanks Dr. C. Zuccaccia, Mr. J.-S. Ryu, Mr. J. A. S. Roberts, Mr. B. D. Stubbart, and Ms. A. M. Kawaoka for helpful discussions.

Supporting Information Available: X-ray crystallographic data, in CIF format, for **10**. This material is available free of charge via the Internet at <http://pubs.acs.org>.

JA0364672